Quantitative model of super-Arrhenian behavior in glass forming materials

J. M. Caruthers and G. A. Medvedev

Phys. Rev. Materials **2**, 055604 — Published 24 May 2018

DOI: 10.1103/PhysRevMaterials.2.055604

A Quantitative Model of Super-Arrhenian Behavior in Glass Forming Materials

J.M. Caruthers and G.A. Medvedev
School of Chemical Engineering
Purdue University
caruther@ecn.purdue.edu and medvedev@ecn.purdue.edu

Abstract
The key feature of glass forming liquids is the super-Arrhenian temperature dependence of the mobility, where the mobility can increase by ten orders-of-magnitude or more as the temperature is decreased if crystallization does not intervene. A fundamental description of the super-Arrhenian behavior has been developed; specifically, the logarithm of the relaxation time is a linear function of $1/\overline{U}_x$, where $\overline{U}_x$ is the independently determined excess molar internal energy and B is a material constant. This one parameter mobility model quantitatively describes data for 21 glass forming materials, which are all the materials where there is sufficient experimental data for analysis. The effect of pressure on the $\log a$ mobility is also described using the same $\overline{U}_x(T,p)$ function determined from the difference between the liquid and crystalline internal energies. It is also shown that B is well correlated with the heat of fusion. The predictions of the $B/\overline{U}_x$ model is compared to the Adam and Gibbs $1/T\overline{S}_x$ model, where the $B/\overline{U}_x$ model is significantly better in unifying the full complement of mobility data. The implications of the $B/\overline{U}_x$ model for the development of a fundamental description of glass are discussed.

I. Introduction

Describing viscosity dependence on temperature for liquids has been a long standing challenge in condensed matter physics. As first pointed out by Andrade,[1] above a characteristic temperature T_A, that depends upon the material, Arrhenian behavior is observed (although Thoms et al[2] recently argued that even at high temperatures this may not hold) as given by

$$\log\left(\frac{\eta}{\eta_0}\right)=\log\left(\frac{\tau}{\tau_0}\right)=\log a_T=\frac{E_A}{RT}-\frac{E_A}{RT_0}\qquad T>T_A \tag{1}$$

where η_0 is the viscosity, τ_0 is the relaxation time at reference temperature T_0, E_A is an activation energy and R is the universal gas constant. At temperatures below T_A the viscosity, or equivalently the relaxation time, undergoes a spectacular increase as the temperature is decreased, where the viscosity increase can be ten or more orders-of-magnitude greater than what would be expected if the high temperature Arrhenian behavior continued to lower temperatures. This super-Arrhenian rise in viscosity with decrease in temperature is one of the key signatures of glass formation. Finally, as the material is cooled further at some temperature the relaxation time exceeds the experimental time and non-equilibrium behavior begins; this results in formation of the glassy state with an associated glass transition temperature T_g. The value of T_g is subjective, since it depends upon the time allowed for equilibration. By convention T_g is defined operationally as the temperature where: (i) the viscosity reaches 10^{13} Pa-s, or (ii) the relaxation time becomes 100s, or (iii) the DSC heat flow exhibits inflection point upon re-heating from the glassy state at the rate of 10K/min, etc.

A number of equations have been proposed to describe the experimentally observed super-Arrhenian mobility data that have been reviewed elsewhere.[3-5] The equations can be divided into two groups: (1) equations that are either purely phenomenological or arise from a derivation that involves experimentally inaccessible quantities so that the end result is an expression with fitting parameters that cannot be independently determined and (2) equations that postulate that $\log a$ is controlled by a specific

thermodynamic variable, where a functional form of $\log a$ expression is then proposed. The most well-known of the phenomenological expressions is the Vogel-Fulcher-Tammann (VFT) equation given by [6-8]

$$\log a_T = \frac{E_{VFT}}{R\left(T - T_{VFT}\right)} - \frac{E_{VFT}}{R\left(T_0 - T_{VFT}\right)} \qquad T_g < T < T_A \tag{2}$$

where T_{VFT} and E_{VFT} are material parameters. The Williams-Landel-Ferry (WLF) equation[9] is equivalent to the VFT equation. Initially T_{VFT} was thought to be the temperature at which a hypothesized phase transition into a glassy state occurs (although it is not observable due to experimental time limitations) and hence the temperature at which the mobility goes to zero. Assuming this postulate to be true, the temperature T_{VFT} would have an objective meaning; however, recently several research groups have presented substantial evidence that the dependence of $\log a$ on temperature may not possess a finite temperature singularity[10,11] – thus, T_{VFT} is just another fitting parameter without physical significance. Moreover, it has been observed that when the experimental mobility range is increased by equilibrating the material at temperatures below the conventional T_g, the parameters T_{VFT} and E_{VFT} change.[12] When the pressure dependence of $\log a$ is included, the parameters T_{VFT} and E_{VFT} have to be made functions of pressure,[13] indicating that Eqn. (2) is a curve fit. Other phenomenological $\log a_T$ equations with two fitting parameters include the proposals of Waterton,[14] (recently resurrected by Mauro et al[15]), Avramov and Milchev,[16] and Elmatad et al[17] and equations with three or more fitting parameters include the proposals of Utracki,[3] Cohen and Grest,[18] Kivelson et al,[19] and Schmidtke et al.[20] Generally the three-parameter equations fit the data well in the entire $T_g \le T \le T_A$ interval for most materials, whereas the two-parameter equations work less well, and depending on the material, they may only fit a portion of the entire $T_g \le T \le T_A$ interval.[3,4,20]

An obvious drawback to the phenomenological approach is that if pressure dependence of the mobility is considered in addition to the temperature dependence, then at least some of the parameters have to be made functions of pressure, resulting in a significant increase in the number of parameters. The situation becomes even worse with regard to describing the non-equilibrium, i.e. glassy, response; where a phenomenological formula, no matter how successful in describing the equilibrium $\log a_T$, provides no clues as to how to predict the sub-T_g mobility. In addition to the effect of temperature and pressure, nonlinear deformation also affects the mobility, where measurements by Ediger and coworkers clearly show that deformation accelerates relaxation.[21] Here again, phenomenological models provide no insight into how $\log a_T$ depends upon deformation, requiring additional deformation dependent parameters.[22]

Historically the first thermodynamic variable postulated to control the mobility in the super-cooled and glassy states was the fractional free volume,[23] where the empirical Doolittle viscosity equation[24] has been used to describe the temperature dependence of $\log a_T$.[25,26] However, the free volume model has serious shortcomings including (i) observation of an isochoric glass transition[27] and (ii) observation of yield in a compressive deformation where the material is densifying and thereby decreasing the free volume, yet the macroscopic mobility dramatically increases.[28] It is of course possible to salvage the free volume models by postulating that the "hard core" volume (used to define the free volume) always behaves in such a way that the agreement with the experimental data is achieved; however, in that case the free volume model becomes just a parameterization of data and should be assigned to the phenomenological class.

Considering the second class of mobility models, a key issue is determination of a thermodynamic variable that can unify the effects of temperature and pressure on $\log a_T$. From the mobility perspective

the glass formation line in temperature-pressure space is an iso-$\log a$ line that is tangent to the experimentally measured dT_g/dp line, where the thermodynamic variable that controls mobility must also be constant along the dT_g/dp line. Using a lattice model, Gibbs and DiMarzio argued that the glass transition is a consequence of the vanishing of configurational entropy at some finite temperature.[29] Configurational entropy is defined as the difference between the liquid entropy (or, more accurately, super-cooled liquid entropy), $\overline{S}_{liq}$, and the glassy entropy, $\overline{S}_{glass}$, i.e. $\overline{S}_c = \overline{S}_{liq} - \overline{S}_{glass}$ (here and in the rest of the paper molar quantities are denoted with an overbar). Although Gibbs and DiMarzio did not propose a particular form of $\log a$, their treatment introduced the idea that configurational thermodynamic quantities control mobility. Goldstein considered the configurational entropy $\overline{S}_c$ and the configurational enthalpy $\overline{H}_c$ as candidates for controlling the glass transition and concluded that they result in the same prediction for the dT_g/dp value.[30] Naoki and Koeda[31] examined several configurational quantities, including $T\overline{S}_c$ and the configurational internal energy $\overline{U}_c$ and found that in case of the glass former orthoterphenyl (OTP) the configurational internal energy gave the value of dT_g/dp that was the closest to experiment. In the papers of Gibbs-DiMarzio, Goldstein, and Naoki-Koeda no explicit functional form of the relationship between mobility and the various configurational thermodynamic quantities was proposed.

In 1965 the pioneering work of Adam and Gibbs (AG) appeared,[32] where mobility in glass forming materials was related to the configurational entropy $\overline{S}_c$. Using the transition state theory (TST)[33-35] with several additional assumptions, Adam and Gibbs proposed:

$$\log a_T = \frac{E_{AG}}{T\overline{S}_c(T)} - \frac{E_{AG}}{T_0\overline{S}_c(T_0)} \tag{3}$$

The parameter E_{AG} is material dependent activation energy. The original meaning of $\overline{S}_c$ as assigned by Adam and Gibbs was the difference between the total entropy and the vibrational contribution to entropy, where they postulated that at a given temperature $\overline{S}_c(T)$ is well approximated by the difference between the super-cooled liquid entropy and the glassy entropy. However, there is no unique glassy entropy, because each glassy state depends on its formation history; consequently, it is better to employ the excess entropy $\overline{S}_x(T) = \overline{S}_{liq}(T) - \overline{S}_{cryst}(T)$, i.e. the difference between liquid and crystalline entropies, which is a well-defined thermodynamic quantity. Thus, the AG $\log a_T$ mobility relationship is more properly given by

$$\log a_T = \frac{E_{AG}}{T\overline{S}_x(T)} - \frac{E_{AG}}{T_0\overline{S}_x(T_0)} \tag{4}$$

However, the crystalline entropy is not available for many materials (including most polymers); thus, the original Adam and Gibbs function, $\overline{S}_c(T)$, is continued to be employed for these materials, where Angell et al. have argued that $\overline{S}_c(T)$ is roughly proportional to $\overline{S}_x(T)$.[36]

Unlike the phenomenological models described above, the AG model given in Eqn. (4) is a one parameter model, provided the $\overline{S}_x(T)$ function is obtained directly from the heat capacity data; however, this is not how the AG model has been historically employed. Prompted by the belief that the empirical VFT equation captures the underlying physics with a divergence in $\log a_T$ at a finite temperature T_2, the configurational entropy or excess entropy has been typically parameterized as

$$\overline{S}_c(T) = \overline{S}_c^{\infty}\left(1 - \frac{T_2}{T}\right) \quad \text{or} \quad \overline{S}_x(T) = \overline{S}_x^{\infty}\left(1 - \frac{T_2}{T}\right) \quad \text{for} \quad T \geq T_2 \tag{5}$$

which forces $\overline{S}_c(T)$ to vanish when $T = T_2$. Substitution of Eqn. (5) into Eqn. (3) results in the VFT expression with $E_{AG}/\overline{S}_c^{\infty} = E_{VFT}/R$ and $T_{VFT} = T_2$. Thus, when the entropy parameterization given in Eqn.

(5) is employed, the resulting AG model has two parameters, $E_{AG}/\overline{S}_x^{\infty}$ and T_2. The VFT form results because (i) Eqn. (5) is a reasonable representation of the experimentally observed behavior for many materials[37] and (ii) there is only a limited range of the liquid and glassy heat capacity data which does not extend below T_g to T_2. The values of $\overline{S}_x^{\infty}$ and T_2 in Eqn. (5) are correlated and thus can often be adjusted while preserving the fit to $\overline{S}_x(T)$ in the range where the heat capacity data exist. This is especially true in case of polymers, where the crystalline heat capacity data are not available and consequently the representation of the configurational entropy using Eqn. (5) inevitably contains adjustable parameters.

Several researchers evaluated the ability of the AG model to fit the $\log a_T$ data in the $T_g \le T \le T_A$ interval. Richert and Angell[38] employed an indirect approach, where the VFT equation was considered as giving an exact representation of the mobility data which was then used to "reverse engineer" the corresponding excess entropy according to Eqn. (4). The computed excess entropy was then compared to the excess entropy obtained from calorimetry data. A reasonably good agreement was reported for several materials for the lower temperature (i.e. closer to T_g) portion of the $T_g \le T \le T_A$ interval, where the model diverged from the data at higher temperatures. A more direct way of testing the AG model is to determine if a $\log a$ vs $1/T\overline{S}_x$ plot is linear, where $\overline{S}_x(T)$ is obtained by straightforward integration of the calorimetry data. This approach was utilized by Magill for tri-α-naphtylbenzene (TNB),[39] by Laughlin and Uhlmann for α-phenyl-o-cresol, salol, and OTP,[40] and recently by Samanta et al for cresolphthalein-dimethylether (CPDE).[41] In all cases the $\log a$ vs $1/T\overline{S}_x$ dependence is not a straight line, but rather a curve of sigmoidal shape (for representative illustrations see Fig. 7 in Laughlin and Uhlmann[40] and Fig. 3 in Samanta et al[41]).

Besides lack of linearity in the AG model when $\log a$ is plotted vs $1/T\overline{S}_x$, there are several additional problems:

1. The AG model predicts the effect of pressure on the mobility as determined by the pressure dependence of the excess entropy. Obtaining such dependence requires pressure-volume-temperature (PVT) data for both the liquid and crystalline phases. To the best of our knowledge the only crystalline PVT data for glass forming liquids is that of Naoki and Koeda for OTP.[31] They found that an iso-$T\overline{S}_x$ condition did not describe the experimentally measured pressure dependence of T_g; however, they did observe that an iso-$\overline{U}_x$ condition provided a better prediction of dT_g/dp. Although all the necessary data was available, Naoki and Koeda did not evaluate the AG model prediction of $\log a$ vs pressure for temperatures other than at T_g.
2. The excess entropy can be lowered isothermally by means of applying a strong electric field to a glass forming material with large dipole moments, where the AG model would then predict a decrease in mobility, i.e. an increase in $\log a$. Recent experiments have detected a small decrease in mobility with an applied electric field; however, the magnitude of this effect is over-predicted by a factor of 4 by the AG model for several small molecular glass formers.[42,43]
3. In the spirit of the original AG derivation and according to Eqn. (5) the maximum possible molar configurational entropy is $\overline{S}_c^{\infty}$ which occurs when $T \to \infty$, where the number of molecules (or repeat units for polymers) in the "cooperatively rearranging region" is by definition equal to 1. Since the minimal number of distinct configurations is two, the value of $\overline{S}_c^{\infty}$ is expected to be $R\ln 2$.[32] Examining the experimental data, for many materials the calculated $\overline{S}_c$ vs T function does not appear to be levelling off as temperature increases, and even if the maximum value exists it significantly exceeds $R\ln 2$.[37] Also, at a lower temperature the number of units in the cooperatively rearranging region is $n(T) = \overline{S}_x^{\infty}/\overline{S}_x(T)$, resulting in n ranging between 4 to 8 in the vicinity of T_g. It is intuitively difficult to rationalize such a small number of units being able to relax without involving any neighboring units.

Notwithstanding the well-documented difficulties detailed in this and the preceding paragraph, the appeal of the AG model has endured for more than fifty years. The primary reason is that the AG model starts from a reasonable molecular hypothesis and results in predictions that capture a number of trends observed experimentally. Moreover, although the aforementioned failures of the AG model are real, the failures are not qualitative, leaving the possibility that the AG model does capture at least some of the underlying physics. In summary the AG model was an ambitious attempt to uncover the underlying physics behind the glass formation phenomena by identifying the thermodynamic quantity that controls mobility – a model that has served the glassy physics community well even though there are known deficiencies

In addition to the effects of temperature, pressure and electric field on the mobility in glass forming liquids, nonlinear deformation is another possible perturbation, where recent measurements by Ediger and coworkers clearly show that deformation accelerates relaxation.[21] Caruthers and coworkers have developed constitutive models of nonlinear viscoelastic response of glassy polymers, where the dominant nonlinearity was the effect of deformation on the mobility.[44] In these constitutive models several versions of $\log a$ functionals were tested with respect to their ability to predict a rich set of thermo-mechanical experiments.[45] It was found that a constitutive model based on the non-linear version of Eqn. (4) was unsatisfactory (in particular the ability to simultaneous predict volume relaxation and yield in both uniaxial extension and compression); however, a constitutive model with reasonable predictions was developed using a $\log a$ functional that depended on the configurational internal energy, $\bar{U}_c$: specifically,

$$\log a = B\left[\frac{1}{\bar{U}_c} - \frac{1}{\bar{U}_{c0}}\right] \tag{6}$$

The configurational internal energy used by Caruthers et al[44] was determined as the current (i.e. the equilibrium internal energy if the current state is an equilibrium liquid or the non-equilibrium internal energy if the current state is glass) internal energy minus the internal energy of the ideal glass. Specifically, $\bar{U}_c = \bar{U} - \bar{U}^{IG} + \bar{\Delta}$, where $\bar{\Delta}$ is a material parameter. The ideal glass energy is by definition the energy of a glassy system, where after formation no structural relaxation occurs. The internal energy $\bar{U}$ includes contributions from both temperature and deformation. Two different classes of constitutive models were investigated, where in both models it was assumed that $\log a$ was controlled by $1/\bar{U}_c$: First, $\bar{U}_c$ was assumed to be a functional of the thermal and deformation history, where the stress, entropy and internal energy functionals were self-consistently determined from an underlying Helmholtz free energy functional;[44] Second, a stochastic constitutive model (SCM) was developed that explicitly incorporated fluctuations consistent with dynamic heterogeneity[46] where local $\bar{U}_c$ was a function of the local and instantaneous entropy and stress as well as of the average temperature and strain. The predictive capabilities of both constitutive models have recently been critically analyzed for an extensive suite of experimental nonlinear thermo-mechanical experiments, where the SCM is the only constitutive model to date that is able to even qualitatively capture the diversity of mechanical data exhibited by polymeric glasses.[47]

The constitutive models described above deal with the non-equilibrium glassy state. Nevertheless, they suggest that mobility model where $\log a$ is a linear function $1/\bar{U}_x$ vs $1/T\bar{S}_x$ as employed in the AG model might provide an effective description of mobility in glass forming liquids in equilibrium state (actually the super-cooled state between T_g and the melting temperature T_m). The objective of this communication is to assess if the $\log a$ mobility can be quantitatively described by the excess internal energy, $\bar{U}_x$, or other excess thermodynamic quantities. In order to (i) critically evaluate this postulate and (ii) determine whether excess quantities can provide an accurate description of the super-Arrhenian mobility, we will

limit this study to materials where there is sufficient high quality thermodynamic data, including thermodynamic data on the crystalline state. In the next section we will first show that for all glass forming liquids where there is sufficient experimental data, the $\log a_T$ mobility data at one atmosphere between T_A and T_g can be accurately described by a linear function of either $1/\overline{U}_x$ or $1/\overline{H}_x$; specifically,

$$\log a_T = \frac{B}{\bar{U}_x(T)} - \frac{B}{\bar{U}_x(T_0)} \tag{7}$$

or

$$\log a_T = \frac{B}{\bar{H}_x(T)} - \frac{B}{\bar{H}_x(T_0)} \tag{8}$$

where $\overline{U}_x$ $(\overline{H}_x)$ is the excess molar internal energy (enthalpy) and B is a material specific constant. In the subsequent section, the effect of pressure on the $\log a$ mobility will be examined, where it will be shown that only the $\overline{U}_x$-based model can describe the pressure effects on $\log a_T$. Finally, we will discuss the relation of the new mobility model to other mobility models and implications for a more fundamental understanding of glass forming liquids.

II. The $\log a_T$ Mobility Model: The Effect of Temperature

II.1 Determination of Excess Thermodynamic Quantities

In order to critically evaluate if $\log a_T$ is a function of $\bar{H}_x$, $\bar{U}_x$, or $T\bar{S}_x$ (or some other excess property) $\bar{H}_x$ and $\bar{S}_x$ must be determined from the liquid and crystalline heat capacity data. The crystalline molar enthalpy at p=p_a=1atm is obtained from experimental heat capacity data as follows:

$$\bar{H}_{cryst}(T, p_a) = \int_0^T \bar{C}_{p,cryst}(T')\,dT' \qquad T \le T_m \tag{9}$$

And the liquid molar enthalpy at p=1atm is obtained similarly as

$$\bar{H}_{liq}(T, p_a) = \bar{H}_{cryst}(T_m, p_a) + \Delta\bar{H}_{fus} + \int_{T_m}^T \bar{C}_{p,liq}(T')\,dT' \qquad T \ge T_m \tag{10}$$

$\bar{C}_{p,liq}\left(\bar{C}_{p,\text{cryst}}\right)$ is the molar constant pressure heat capacity of the liquid(crystal) at p=1atm; $\Delta\bar{H}_{fus}$ is the molar enthalpy of fusion; and, T_m is the melting temperature at p=1atm. It is not required that the integration in Eqn. (9) begin at absolute zero, where any temperature that is lower than the temperature of interest will suffice, since the excess enthalpy will not depend upon where the integration begins. For liquids at p=1atm there is negligible difference between $\bar{H} = \bar{U} + p\bar{V}$ and $\bar{U}$; thus, the $\log a_T$ mobility at p=1atm can be in terms of either the excess internal energy, i.e. Eqn. (7), or excess enthalpy, i.e. Eqn. (8). The excess enthalpy needs to be evaluated for the temperature interval $T_g \le T \le T_A$ (or even below the conventional T_g if corresponding experimental data for equilibrated material is available). Considering that typically the melting temperature T_m is located somewhere in the middle of this interval, extrapolations are required. Then Eqn. (9) becomes

$$\bar{H}_{cryst}(T, p_a) = \int_0^T \bar{C}^{extrap}_{p,cryst}(T')\,dT' \qquad T > T_m \tag{11}$$

Similarly, in case of a super-cooled liquid we use Eqn. (10) with the super-cooled liquid molar heat capacity $\bar{C}_{p,sc\,liq}$, i.e.

$$\bar{H}_{liq}(T,p_a)=\bar{H}_{cryst}(T_m,p_a)+\Delta\bar{H}_{fus}+\int_{T_m}^{T}\bar{C}_{p,sc\,liq}(T')\,dT' \qquad T<T_m \tag{12}$$

Combining Eqns. (9-11) and (10-12), the excess molar enthalpy at p=1atm for the temperature interval of interest is given by

$$\bar{H}_x(T,p_a)=\bar{H}_{liq}(T,p_a)-\bar{H}_{cryst}(T,p_a) \tag{13}$$

Analogously, the crystalline and liquid entropies are calculated as (where extrapolations are implied if necessary)

$$\bar{S}_{cryst}(T,p_a)=\int_{0}^{T}\frac{\bar{C}_{p,cryst}(T')}{T'}dT' \tag{14}$$

and

$$\bar{S}_{liq}(T,p_a)=\bar{S}_{cryst}(T_m,p_a)+\Delta\bar{S}_{fus}+\int_{T_m}^{T}\frac{\bar{C}_{p,liq}(T')}{T'}dT' \tag{15}$$

where $\Delta\bar{S}_{fus}$ is the molar entropy of fusion. The enthalpy and entropy of fusion are related via $\Delta\bar{S}_{fus}=\Delta\bar{H}_{fus}/T_m$. The excess molar entropy at p=1atm is

$$\bar{S}_x(T,p_a)=\bar{S}_{liq}(T,p_a)-\bar{S}_{cryst}(T,p_a) \tag{16}$$

The internal energy (at all pressures) is obtained using the standard thermodynamic relation as

$$\bar{U}_x(T,p)=\bar{H}_x(T,p)-p\bar{V}_x(T,p) \tag{17}$$

where $\bar{V}_x(T,p)=\bar{V}_{liq}(T,p)-\bar{V}_{cryst}(T,p)$ is the excess molar volume and $\bar{V}_{liq}\left(\bar{V}_{cryst}\right)$ is the liquid(crystalline) molar specific volume. Once $\bar{H}_x$ and $\bar{S}_x$ are determined from the experimentally measured heat capacity and enthalpy of fusion, then all other excess thermodynamic quantities are determined using standard thermodynamic relationships, e.g. $\bar{G}_x=\bar{H}_x-T\bar{S}_x$.

There are three challenges to test the relationships given in Eqns. (4) and (8), which also serve as the criteria for including a particular material in the subsequent analysis:

1. There needs to be mobility data that extends from conventional T_g to high enough temperatures so that T_A can be determined, since the postulated (super-Arrhenian) relationship between excess thermodynamic quantities and $\log a_T$ should only be valid between T_g and T_A. Typically $\log a_T$ changes by 12 orders-of-magnitude between T_g and T_A. Also, 1 to 2 orders of magnitude of the $\log a_T$ range are needed to robustly determine the Arrhenian behavior above T_A. This means that at least 13 orders of magnitude of the mobility data are required, thereby excluding a large number of materials for which only 5 to 6 orders-of-magnitude of $\log a_T$ are available.
2. Heat capacity data is needed for the crystalline state. Thus, materials that do not crystallize (usually because they exist in the form of two or more isomers) have to be excluded even though ample mobility data in the super-cooled state are available. Two examples are dibutylphthalate[48] and propylene glycol.[49] Also, for most materials the melting temperature T_m lies below T_A, which means that the temperature dependence of the crystalline heat capacity needs to be extrapolated in the T_m to T_A range. Based upon our experience during the course of the analysis reported in this paper, we believe that data from adiabatic calorimetry is preferred, where the more common DSC

data may not have sufficient accuracy. Finally, accurate determination of the enthalpy of fusion, $\Delta\overline{H}_{fus}$, is critically important.

3. Determination of excess thermodynamic quantities requires subtraction of the crystalline heat capacity from the liquid heat capacity, where direct subtraction of data is only possible if the material can be super-cooled well below T_m. For several glass formers preventing partial crystallization is challenging, in which case the DSC data may prove more accurate as compared to the adiabatic calorimetry data due to the long time scale (and hence the possibility for crystallization) involved in the latter technique. An example of material that had to be excluded despite existence of high quality mobility data[50] as well as crystalline and liquid (but not super-cooled liquid) heat capacity data[51] is α–picoline.

The three constraints above limit the number of materials that can be critically evaluated; in particular, clean thermodynamic characterization of the crystalline state for polymers is difficult. Specifically, issues concerning crystallization kinetics, molecular weight effects and crystallite morphology make determination of the crystalline enthalpy and entropy problematic. The exception to this is polyethylene (LDPE), for which the crystalline properties are well established;[52] although, the available mobility data are via dielectric spectroscopy, where LDPE material needed to be doped with molecules with large dipole moment to boost the signal and where the $\log a_T$ range was less than 7 decades.[53] Thus, polymers have not been included in the initial study reported in this paper. Also not included are the complicated cases of small molecule glass formers, for which multiple crystalline phases (e.g. ethanol[54-56]) and/or multiple glass transitions (e.g. MTHF[57]) have been reported. Notwithstanding these challenges in accurately determining the excess thermodynamic quantities, there are 21 small molecules where there the needed heat capacity and mobility data are available.

The mobility data for glass forming materials come in several forms; specifically, measurements include the absolute values of the relaxation times (e.g. NMR), frequencies (e.g. loss peak position in dielectric spectroscopy) or the viscosities; in other cases only the $\log a_T$ shifts required for time-temperature superposition are available. Relating and comparing the results of different experimental methods has been an active area of research in the glass field, which potentially has fundamental implications. Having acknowledged that, for the purpose of this paper, where the temperature dependence of mobility is the primary focus, we cast all data in the $\log a_T$ vs T form and apply a vertical shift to achieve best possible overlap between the different types of data. Our goal in what follows is not a comprehensive review of all mobility data for each of the 21 materials. As a result, some of the data for a given material may have been omitted. An example would be a single temperature point measurements, which can always be vertically shifted to lie on the existing $\log a_T$ vs T curve without adding any new information. With these caveats we believe that the data compiled for each of the 21 glass forming materials described in both the next section and in the Supporting Information[58] represents the best $\log a_T$ vs T data available for glass forming materials.

II.2 Ortho-terphenyl (OTP).

Ortho-terphenyl is one of the most studied small molecule glass formers, where the mobility has been determined by a variety of experimental methods including viscosity,[40,59-62] dielectric relaxation,[63] photon correlation spectroscopy,[64] and light scattering using a tandem Fabry-Perot interferometer.[64] The $\log a_T$ vs T data are for the temperature interval from 239K to 555K as shown in Fig. 1A. We use the common designation in the glass literature that a super-cooled material is an *equilibrium* liquid between T_m and T_g even though the true equilibrium state would be the crystal. The $\log a_T$ data spans 16 orders-of-magnitude, where the viscosity and spectroscopic data are in good agreement. The temperature dependence of the mobility exhibits Arrhenian behavior at temperatures above T_A=401K and super-Arrhenian behavior below T_A. The conventional T_g is 243K (as determined by DSC on heating at 10K/min), although the equilibrium mobility data are available down to 239K at which point further equilibration becomes impractical. The mobility at the lowest temperature is approximately 13 orders-of-magnitude lower (i.e. $\log a_T$ is higher) than what would be expected based upon extrapolation of the high

temperature Arrhenian response. It should be noted that, although a definite value for T_A is given in this paragraph and in Table 1, there is a cross-over region between the Arrhenian and super-Arrhenian behaviors, resulting in an uncertainty in T_A of ±5K at 401K.

The heat capacity data[65] for OTP are shown in Fig. 1B, where the crystalline data are available to 2.34K (but not shown). The melting transition for OTP occurs at 329.35K, which is between the green and red symbols in Fig. 1B. Data points affected by pre-melting phenomena (possibly due to presence of impurities) have been discarded. The heat capacity data are interpolated using 1st and 3rd order polynomials (the latter is the lowest order polynomials providing a uniformly good fit to the liquid heat capacity data) with the coefficients given as follows:

$$C_{p,cryst} = 0.960 \cdot T - 11.63 \quad \left(J\ mol^{-1}\ K^{-1}\right) \tag{18}$$

$$C_{p,liq} = -2.82 \cdot 10^{-6} \cdot T^3 + 2.92 \cdot 10^{-3} \cdot T^2 - 0.351 \cdot T + 288.5 \quad \left(J\ mol^{-1}\ K^{-1}\right) \tag{19}$$

These same polynomials are used to extrapolate the values of the heat capacities to the entire region between T_g and T_A as needed to predict the $\log a_T$ data. Obviously, such an extrapolation (shown as dashed lines in Fig. 1B) is not based on any physical mechanism, but it does not appear unreasonable within the relatively limited range of temperatures in the above T_m region. The parameterization of the heat capacities given in Eqns. (18) and (19) are used to determine the entropy and the enthalpy in the crystalline and the liquid states via integration according to Eqns. (9), (10), (12) and (13). The entropy of fusion ($\Delta S_{fus} = 52.20$ J mol^{-1} K^{-1}) and the enthalpy of fusion ($\Delta H_{fus} = 17191$ J mol^{-1}) are also from Chang and Bestul.[65] Subsequently the excess entropy and excess enthalpy are determined and shown in Fig. 1C. As expected the $T\bar{S}_x$ and $\bar{H}_x$ curves intersect at T_m, where $\bar{H}_x - T\bar{S}_x = \bar{G}_x = 0$. The $T\bar{S}_x$ curve is very close to a straight line demonstrating that, in case of OTP and for the temperature range in question, Eqn. (5) is a good approximation for $\bar{S}_x$, whereas $\bar{H}_x$ is curved. If the $T\bar{S}_x$ curve is linearly extrapolated to lower temperatures (although there is no known physical reason that the temperature dependence should be linear well below T_g) it will reach zero at some finite temperature. However, the validity of a linear extrapolation of $T\bar{S}_x$ or $\bar{H}_x$ to lower temperatures is of no significance in the current analysis of materials at equilibrium, where the mobility data will only be analyzed for temperatures greater than T_g .

To test the validity of the single-parameter models given in Eqns. (4) and (8), the OTP $\log a_T$ data at p=1atm are plotted vs $1/T\bar{S}_x$ in Fig. 1D and $1/\bar{H}_x$ in Fig. 1E. Examining Fig. 1D, the $1/T\bar{S}_x$ mobility model clearly fails to linearize the $\log a_T$ data, where the curve is slightly sigmoidal (to visually emphasize the deviation from linearity a straight line is shown in Fig. 1D). Alternatively, as evidenced by Fig. 1E the $1/\bar{H}_x$ model linearizes the $\log a_T$ data over 12.7 logarithmic decades within experimental uncertainty; the corresponding fit to the $\log a_T$ vs T data using Eqn. (8) is shown in Fig. 1A as a solid line with a value of B=233.3 kJ/mole. The temperature range for which the Eqn. (8) results in a good fit to the $\log a_T$ data is from 239K to 304K. For the rest of the temperature interval of interest (i.e. from 304K to T_A = 401K) the Eqn. (8) model departs from the data as seen in both Fig. 1A and Fig. 1E. The $\log a_T$ range exhibiting a crossover from the $1/\bar{H}_x$ mechanism to the standard Arrhenian temperature dependence observed above T_A is 2.3 logarithmic decades.

At p=1atm the difference between $\bar{H}_x = \bar{U}_x + p_a\bar{V}_x$ and $\bar{U}_x$ is insignificant; thus, $\log a_T$ is also a linear function of $1/\bar{U}_x$. However, at elevated pressures there will be a difference between $\bar{H}_x$ and $\bar{U}_x$ which will be analyzed in the next Section. Other excess thermodynamic quantities like the molar Helmholtz or Gibbs free energy as well as other simple functional forms like $\log a_T$ vs $\bar{H}_x$ were considered, but they were unable to describe the mobility data with accuracy comparable to the $1/\bar{H}_x$ model. Of course more complicated mobility models involving excess thermodynamic quantities could also possibly describe the

data, but why would one employ a more complex $\log a_T$ model with multiple fitting parameters when the one parameter $1/\bar{H}_x$ model does such an excellent job?

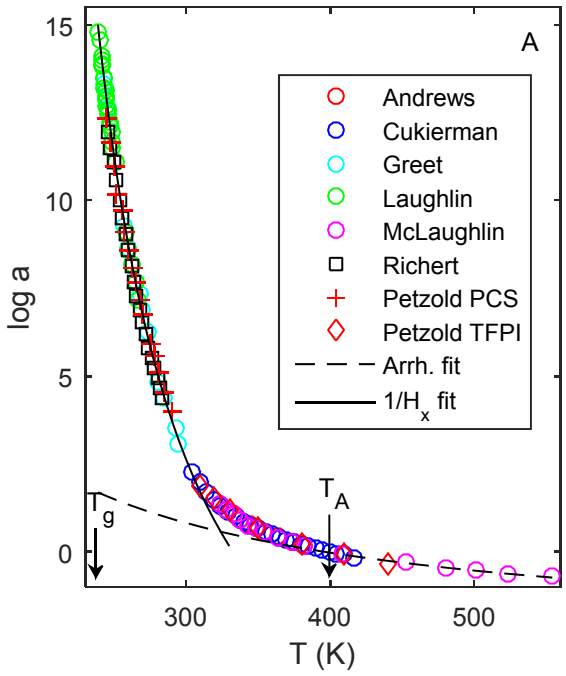

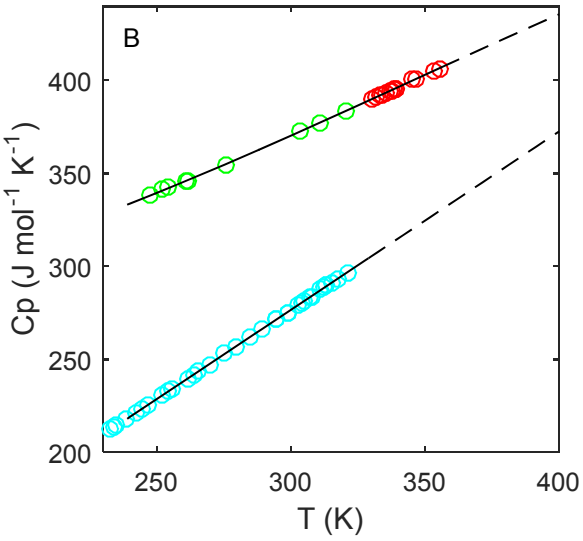

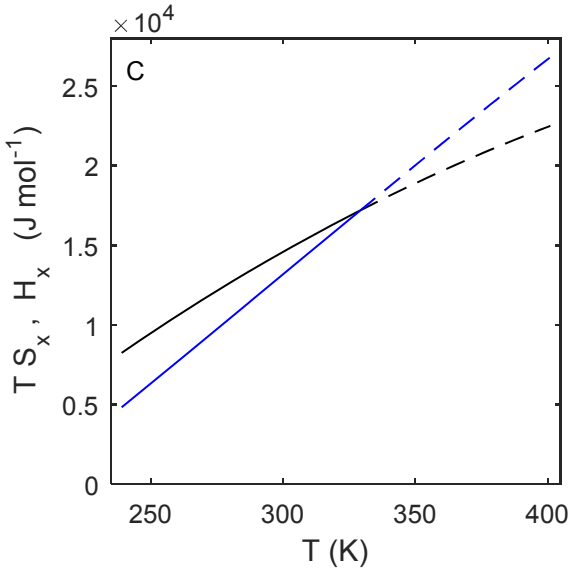

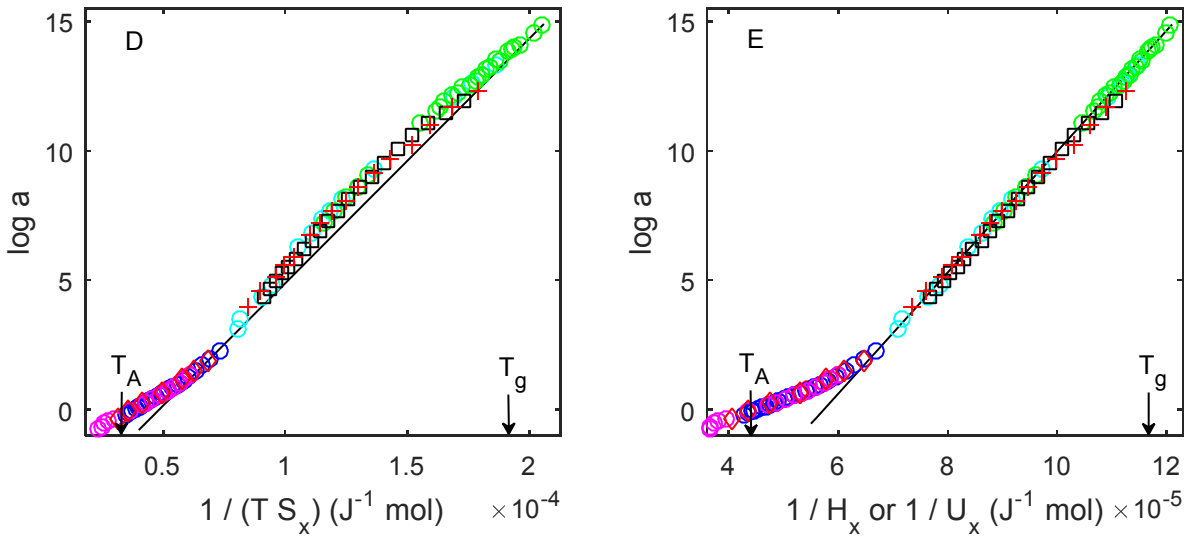

Figure 1. Analysis of OTP data. (A) Mobility data including viscosity (Andrews and Ubbelodhe,[59] Cukierman et al,[60] Greet and Turnbull,[61] Laughlin and Uhlmann,[40] and McLaughlin and Ubbelodhe[62]), dielectric relaxation (Richert[63]), photon correlation spectroscopy and the light scattering (Petzold and Rossler[64]) data. The dashed line is the high temperature Arrhenian response and solid line is the prediction of the $B / \bar{H}_x$ model. The reference state is $\log a(T_A, p_a) = 0$; (B) Heat capacity data in the T_g to T_a range is from Chang and Bestul:[65] cyan circles – crystal, red circles – equilibrium liquid, green circles – super-cooled liquid. Solid lines are interpolations and dashed lines are extrapolations of the data (see text); (C) Excess $1 / T\bar{S}_x$ (blue) and excess $1 / \bar{H}_x$ (black) calculated from the data in Fig. 1B, where dashed portions of the curves correspond to temperatures where crystalline and liquid heat capacities were extrapolated; and, mobility data vs. (D) $1 / T\bar{S}_x$ and (E) $1 / \bar{H}_x$ or $1 / \bar{U}_x$, where the symbols are the same as in Fig. 1A. In (D) the solid straight line is a guide to the eye, while in (E) the solid line is a linear fit with the slope B=233.3 kJ/mole.

II.3 m-Toluidine

The mobility in the super-cooled region of small molecule glass former m-toluidine has also been analyzed. The temperature dependence of $\log a_T$ at p=1atm is shown in Fig. 2A which includes viscosity,[66,67] mechanical,[68,69] dielectric,[10,70-72] light scattering,[67,71] and NMR[66] mobility data. There are some discrepancies in the data especially at temperatures above T_A, although they are not apparent in Fig. 2A (see Figs. 2D and 2E, where the discrepancies are magnified). The $\log a_T$ vs T data are for the temperature interval from 181K to 473K which span nearly 16 decades of $\log a_T$. The T_g as determined via DSC is 187K.[73] The $\log a_T$ vs T dependence is Arrhenian (shown as dashed line in Fig. 2A) from the maximum available temperature of 473K down to T_A=275K, after which the super-Arrhenian behavior begins. Thus, the Arrhenian $\log a_T$ range is approximately 2 decades and the super-Arrhenian range is at least 14 decades. The reference temperature (i.e. where $\log a_T$=0) in Fig. 2A is chosen at T_A. The mobility at T_g is approximately 12 orders-of-magnitude lower than would be expected based upon the high temperature Arrhenian response.

The heat capacity data for m-toluidine are shown in Fig. 2B for the temperature range of interest. Unlike in case of OTP where the adiabatic calorimetry data were available, the data of Alba-Simionesco et al[73] are from DSC measurements. The heat capacity data are interpolated using polynomials with the coefficients given as follows:

$$C_{p,cryst} = 1.06 \cdot 10^{-4} \cdot T^3 - 5.81 \cdot 10^{-3} \cdot T^2 + 10.9 \cdot T - 596.0 \quad \left(J\ mol^{-1}\ K^{-1} \right) \tag{20}$$

$$C_{p,liq} = 0.137 \cdot T + 176.1 \quad \left(J\ mol^{-1}\ K^{-1} \right) \tag{21}$$

These polynomials are used to determine the values of the heat capacities over the entire T_g to T_A interval as necessary to predict the $\log a_T$ vs T data, which include extrapolations of the crystalline heat capacity above T_m. Obviously, such an extrapolation (shown as dashed lines in Fig. 2B) is not based on any physical mechanism, but it does not appear unreasonable within the range of interest. The melting transition for m-toluidine occurs at 241.65K, where the entropy of fusion ($\Delta S_{fus} = 36.0$ J mol^{-1} K^{-1}) and the enthalpy of fusion ($\Delta H_{fus} = 8.8$ kJ mol^{-1}) were determined by Meva'a and Lichanot.[74] The parameterizations of the heat capacities given in Eqns. (20) and (21) were used to determine the entropy and the enthalpy in the crystalline and the liquid states via integration according to Eqns. (9), (10), (12), and (13). The excess entropy and excess enthalpy determined are shown in Fig. 2C. As expected the $T\bar{S}_x$ and $\bar{H}_x$ curves intersect at T_m. Unlike the case for OTP, the $T\bar{S}_x$ vs T is not linear, but exhibits a slight upward curvature.

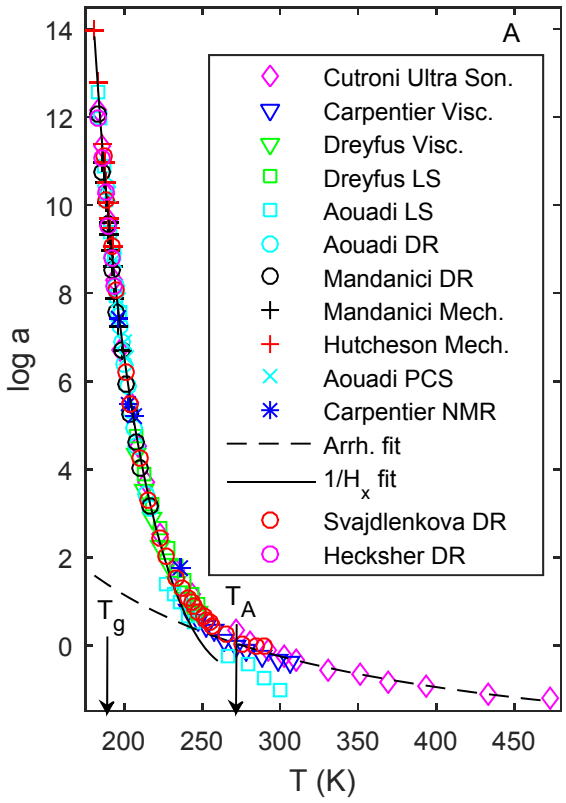
A
log a
T (K)
Cutroni Ultra Son.
Carpentier Visc.
Dreyfus Visc.
Dreyfus LS
Aouadi LS
Aouadi DR
Mandanici DR
Mandanici Mech.
Hutcheson Mech.
Aouadi PCS
Carpentier NMR
Arrh. fit
1/H_x fit
Svajdlenkova DR
Hecksher DR
T_g
T_A

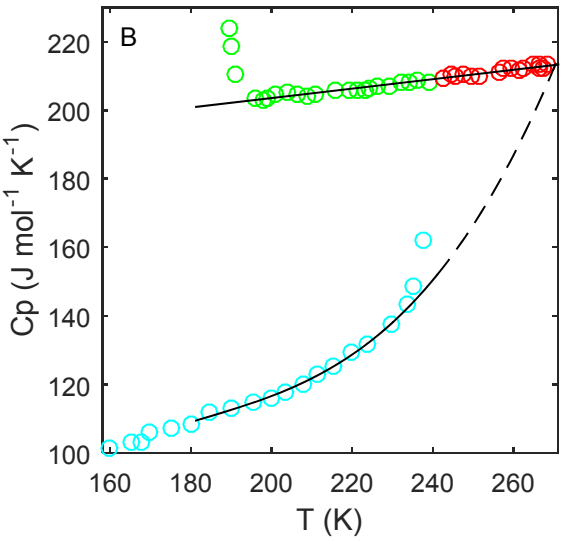
B
Cp (J mol^-1 K^-1)
T (K)

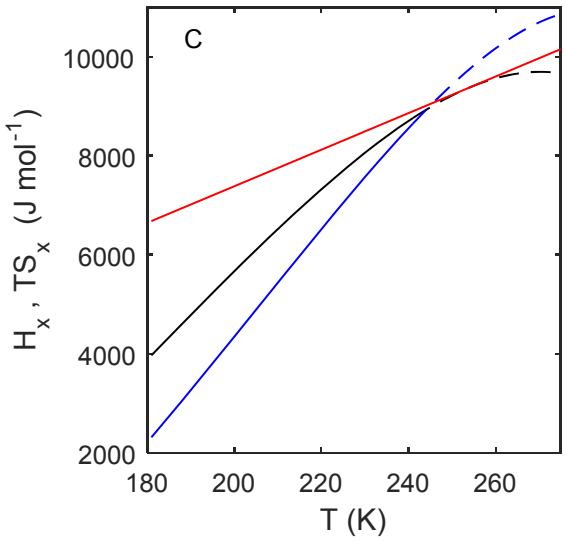
C
H_x , TS_x (J mol^-1)
T (K)

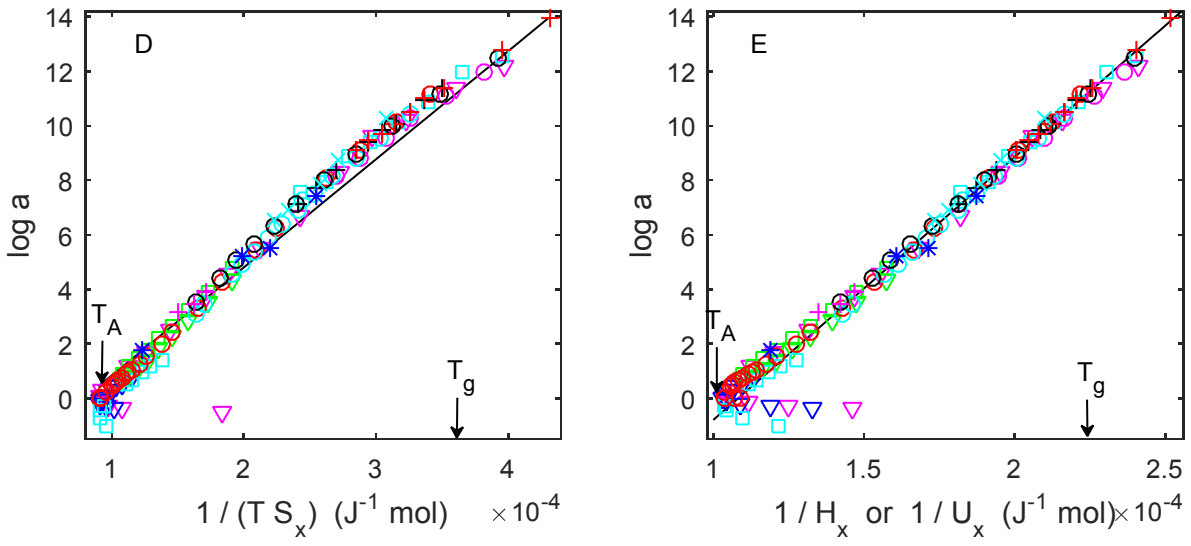

Figure 2. Analysis of m-toluidine data. (A) Mobility data including ultrasonic (Cutroni and Mandanici[69]), viscosity (Carpentier et al,[66] Dreyfus et al[67] and references within), mechanical relaxation (Cutroni and Mandanici,[69] Hutcheson and McKenna[68]), dielectric relaxation (Aouadi et al,[71] Mandanici et al,[70] Hecksher et al,[10] and Svajdlenkova et al[72]) light scattering (Dreyfus et al,[67] Aouadi et al[71]), photon correlation spectroscopy (Aouadi et al[71]) and NMR data (Carpentier et al[66]). The dashed line is the high temperature Arrhenian response and solid line is the prediction of the $B/\bar{H}_x$ model. The reference state is $\log a(T_A, p_a) = 0$; (B) Heat capacity data in the T_g to T_A range are from Alba-Simionesco et al:[73] cyan circles – crystal, red circles – equilibrium liquid, green circles – super-cooled liquid. Solid lines are interpolations and dashed lines are extrapolations of the data (see text for details). (C) Excess $1/T\bar{S}_x$ (blue) and excess $1/\bar{H}_x$ (black) calculated from the data in Fig. 2B, where dashed portions of the curves correspond to temperatures where crystalline and liquid heat capacities were extrapolated, red line is the asymptote to H_x vs. T line at temperatures above T_m given by $H_x = 36.6\left(J \cdot mol^{-1} \cdot K^{-1}\right) \cdot T$ (see Discussion); and, (D) mobility data vs $1/T\bar{S}_x$ and (E) mobility data vs $1/\bar{H}_x$ or $1/\bar{U}_x$, where the symbols are the same as in Fig. 2A. In (D) the solid straight line is a guide to the eye, while in (E) the solid line is a linear fit to the data with the slope B=87.7 kJ/mole.

The $\log a_T$ mobility data vs $1/T\bar{S}_x$ is shown in Fig. 2D, where the $\log a_T$ response is not linear but rather is a sigmoidal function of $1/T\bar{S}_x$, where to visually emphasize the deviation from linearity a straight line is shown in Fig. 2D. Finally, a plot of $\log a_T$ vs $1/\bar{H}_x$ is shown in Fig. 2E, where within experimental uncertainty $\log a_T$ is a linear function of $1/\bar{H}_x$ over 12 logarithmic decades with a slope of B=96.4 kJ/mole. The temperature range, for which $\log a_T$ is a linear function of $1/\bar{H}_x$ is from 181K to 225K, i.e. from below T_g to the crossover region to Arrhenian behavior. The $\log a_T$ range exhibiting the crossover from $1/\bar{H}_x$ to Arrhenian behavior is relatively narrow, being less than two logarithmic decades. The data shown in Fig. 2 for m-toluidine clearly demonstrate that the $1/\bar{H}_x$ (or equivalently $1/\bar{U}_x$ for p=1am data) is a better model of the super-Arrhenian response than $1/T\bar{S}_x$, when the excess thermodynamic quantities are computed directly from heat capacity data in the super-cooled region without an extrapolation that assumes a specific functional form for the temperature dependence of $\bar{C}_p$.

In Fig. 2E the Arrhenian response for $T > T_A$ are the nearly horizontal data points that have a *negative* slope with respect to $1/\bar{H}_x$. This is in contrast to the response in the Arrhenian region for OTP shown in

Fig. 1E, where the slope of $\log a$ vs. $1/\bar{H}_x$ is positive. The unanticipated high temperature response exhibited by m-toludine is a direct result of the significant curvature in the crystalline heat capacity data as T approaches T_m shown in Fig. 2B, which is then extrapolated into the Arrhenian region above T_m. The extrapolation of highly curved heat capacity data is problematic, where the negative slope of the $\log a$ vs. $1/\bar{H}_x$ m-toludine data at high temperatures may be an artifact of the extrapolation. Even though the high temperature m-toludine $\log a$ vs. $1/\bar{H}_x$ is in question, there are no such extrapolation problem below T_A, where the data clearly show that $\log a$ is a linear function of $1/\bar{H}_x$

II.4 Super-Arrhenian Response of Other Glass Forming Liquids

The analysis in the previous two sections for OTP and m-toluidine showed that the super-Arrhenian $\log a_T$ response at p = 1 atm is a linear function of $1/\bar{H}_x$ (or equivalently $1/\bar{U}_x$). A similar analysis of the super-Arrhenian response of an additional 19 glass forming materials was performed, where the detailed analysis for each material is given in the Supporting Information[58]. We believe that these 19 glass forming materials along with OTP and m-toluidine are the only materials where there is sufficient thermodynamic and $\log a_T$ mobility data for a critical analysis

The analysis summarized in Fig. 3 involved the synthesis of considerable amount of data which is discussed in detail in the Supporting Information[58], where for a single material it could involve multiple research groups over decades, e.g. for m-toluidine as reported in Fig. 2 there were 12 different measurements of mobility. For the materials shown in Figs. 3A-D the $\log a_T$ vs $1/\bar{H}_x$ plot is linear for more than 10 orders-of-magnitude, with the exception of 3-Bromopentane, ethylbenzene, dimethyphthalate, and tiphenylphosphite for which there is a sizable gap of up to 4 orders-of-magnitude in the $\log a_T$ data: nevertheless, the linearity is not in doubt. There are four other materials where either (i) the linearity of the fit is not as good or (ii) the range of linearity is less. Importantly, even for these "problematic" materials the $1/\bar{H}_x$ model does not fail; rather, the observed discrepancies indicate potential issues with the data, which in turn have objective causes. Specifically, (see the Supporting Information[58] for more detailed information including references):

1. Toluene and Ethyl benzene. Toluene and ethyl benzene have a tendency to crystallize in the super-cooled state; consequently, in order to measure $\bar{C}_{p,liq}$ for the super-cooled liquid state for these compounds Yamamuro et al[37] resorted to doping them with 10% benzene. The desired value of $\bar{C}_{p,liq}$ for the pure material was obtained under the assumption that the contributions were additive. The validity of such assumption cannot be independently evaluated, so the heat capacity and hence the enthalpy data for these materials are suspect. In case of toluene significant scatter in the mobility data in the 122K to 130K range exists, which may be related to partial crystallization. In addition, two different crystalline phases have been reported for toluene, where it is unclear if they have the same melting temperature and the enthalpy of fusion.[75] Thus, there is uncertainty concerning if the correct enthalpy of fusion is used to generate the prediction in Figs. 3C and 3D.
2. Propylene carbonate. Two substantially different melting temperatures and corresponding enthalpies of fusion have been reported.[76,77] This could possibly be the result of enantiomer mixtures, where different samples have different compositions. It is not known if this difference in melting points would also affect the mobility data, which was determined by different research groups.[78-81]
3. Glycerol. An unknown amount of crystallization was reported as occurring in the super-cooled state depending on the thermal history;[82,83] thus, $\bar{C}_{p,liq}$ for the super-cooled liquid may not be reliable.

These four materials are marked with a star in Table 1, where the values of parameter B should be considered as preliminary. Note also that in case of toluene, glycerol, and sorbitol the $1/T\bar{S}_x$ (i.e. AG) model fails badly as shown in the Supporting Information[58]. In case of propylene carbonate the $\log a_T$ vs $1/\bar{H}_x$ plot has a slight curvature as shown in Fig. 3D whereas $\log a_T$ vs $1/T\bar{S}_x$ plot appears more linear as shown in the Supporting Information[58].

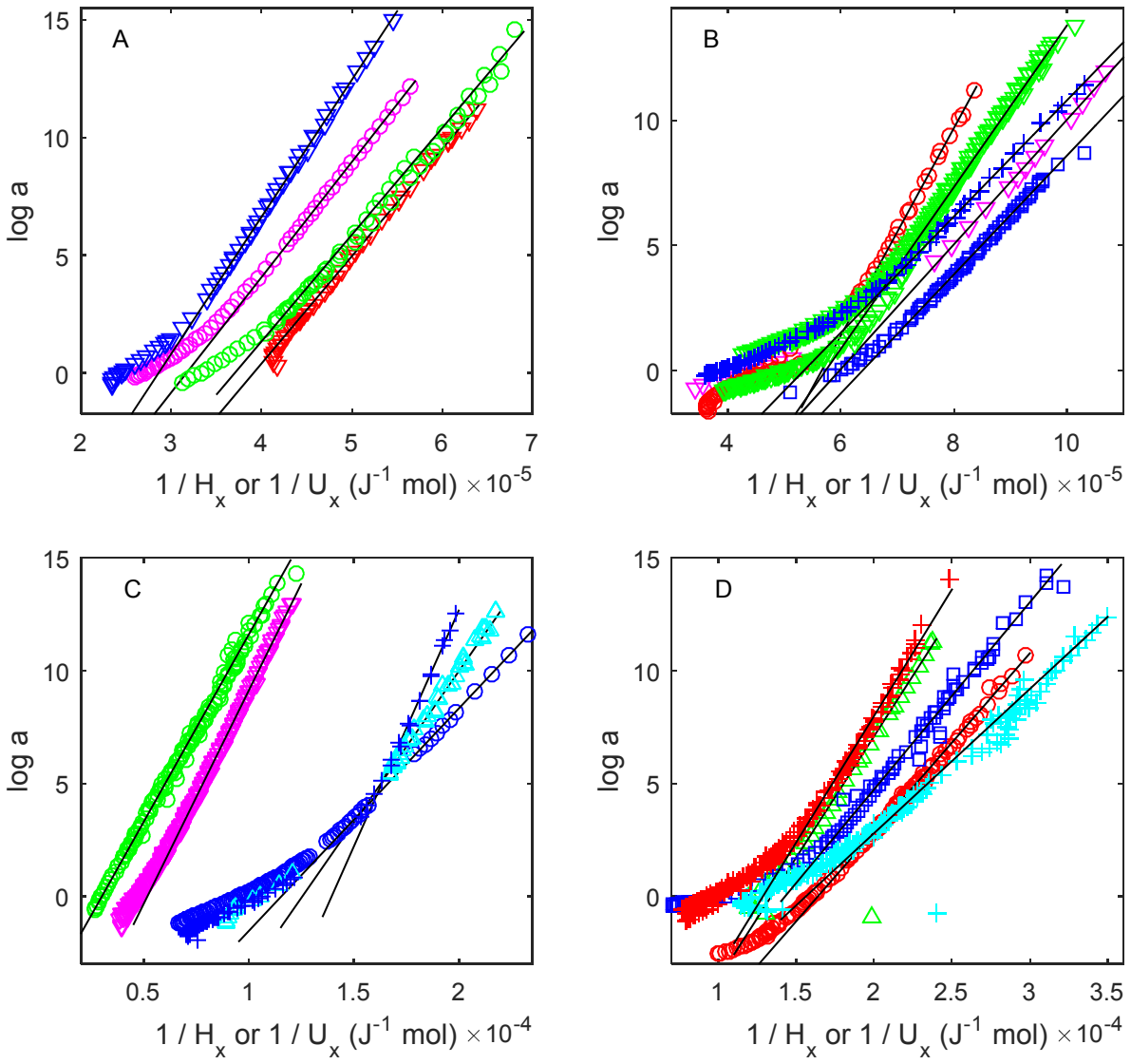

Figure 3. $\log a_T$ mobility vs $1/\bar{H}_x$ or equivalently $1/\bar{U}_x$ for a series of glass forming liquids at p = 1atm. (**A**) Tri-α-naphtylbenzene (TNB) – blue triangles; Cresolphthalein-dimethylether (CPDE) – magenta circles; Glucose (Glu) – green circles; B_2O_3 – red triangles; (**B**) α-Phenyl-o-cresol (o-benzylphenol) (oBP) – blue pluses; Diethyl phthalate (DEP) – blue squares; Dimethyl phthalate (DMP) – magenta triangles; Triphenyl phosphite (TPP) – red circles; Salol (Sal) – green triangles; (**C**) Sorbitol (Sor) – green circles; Glycerol (Gly) – magenta triangles; Ethylcyclohexane (ECH) – blue circles; Ethyl benzene (EB) – blue pluses; 3-Bromopentane (3BP) – cyan triangles; (**D**) 3-Methylpentane (3MP) – blue squares; n-Propanol (nProp) – red circles; Cumene (isopropylbenzene) (iPB) – green triangles; Toluene

(Tol) – cyan pluses; Propylene carbonate (PC) – red plusses.. The sources of all mobility data are given in the Supporting Information[58].

Notwithstanding the concerns discussed above, the mass of data indicate that $\log a_T$ in the super-Arrhenian region is a linear function of $1/\bar{H}_x$. In addition, in our experience the higher the overall robustness of the mobility and thermodynamic data the better is the performance of the $1/\bar{H}_x$ model. For all the materials shown in Fig. 3, at higher temperatures (and thus higher values of $\bar{H}_x$) there is both (i) an Arrhenian response (i.e. for $\log a_T$ values below $\log a_T = 0$, which is the reference state at T_A and p=1atm) and (ii) a cross-over region between the Arrhenian and super-Arrhenian response, where $\log a_T$ is not a linear function of $1/\bar{H}_x$. The $\log a_T$ range of this cross-over region is less than 3 orders-of-magnitude for the materials in Fig. 3 (except for the four materials with the gap in the mobility data mentioned above, for which the size of the cross-over region cannot be established). The materials shown in Fig. 3, for which the cross-over region is larger, are the materials for which the mobility and especially the heat capacity data are less certain leaving the possibility that once the questions regarding the data are resolved, the linearity range will extend and the cross-over region will shrink (see the sensitivity analysis in the next Section). The slope B in the $\log a_T \sim B/\bar{H}_x$ model is given in Table 1 along with additional data for each of the glass forming materials analyzed, including T_g, the range of $\log a_T$ data, T_A, the activation energy, $\bar{E}_A$, for the high temperature Arrhenian response, the melting point T_m and the enthalpy of fusion $\Delta\bar{H}_{fus}$. The data in Fig. 3 clearly shows that $\log a_T$ at p=1atm is a linear function of $1/\bar{H}_x$ (or equivalently $1/\bar{U}_x$) for all materials where there is thermodynamic and mobility data of sufficient quality for analysis.

Because of the prominence of the Adam-Gibbs model for describing the super-Arrhenian $\log a_T$ response, $\log a_T$ vs $1/T\bar{S}_x$ was also analyzed for all the materials in Table 1. For most of the material $\log a_T$ vs $1/T\bar{S}_x$ exhibited sigmoidal curvature like that shown for OTP and m-toluidine in Figs. 1 and 2 (see Supporting Information[58] for details). However, for three materials $\log a_T$ was a linear function of $1/T\bar{S}_x$: ethylbenzene, propylene carbonate, and dimethyl phthalate. The relationship between $\bar{H}_x$ and $T\bar{S}_x$ is given by $\bar{G}_x = \bar{H}_x - T\bar{S}_x$; thus, if $\bar{G}_x$ is small, then $\bar{H}_x \approx T\bar{S}_x$, where $1/T\bar{S}_x$ exhibits a linear response if $1/\bar{H}_x$ exhibited a linear response. Thus, $1/T\bar{S}_x$ mobility model does describe the $\log a_T$ response for a few materials (although the $1/\bar{H}_x$ model works equally well for these materials); however, when considering all the glass forming materials given in Table 1, the $1/\bar{H}_x$ model is a significantly better description of the super-Arrhenian behavior.

Table 1. Material Properties and $1/\bar{H}_x$ Model parameters for 21 Glass Forming Materials

Material	T_g (K)	$\log a_T$ data range (K)	T_A (K)	$\bar{E}_A$ (kJ/mol)	T_m (K)	$\Delta\bar{H}_{fus}$ (kJ/mol)	B (kJ/mol)	λ	$\frac{B}{\lambda}$ (kJ/mol)	$\frac{B}{\lambda\bar{E}_A}$
3-Methyl pentane	77	76-427	212	2.65	110.25	5.3	82.9	5.8	14.4	5.4
n-Propanol	98	99-369	183	7.7	148.81	5.40	79.15	4.3†	18.4†	2.4†
Ethyl cyclohexane	104	103-384	212	4.65	161.8	8.3	98.6	6.2	15.9	3.4
3-Bromo pentane	108	107-298	194	5.6	167.3	8.40	134.0	6.05	22.2	4.0

Ethylbenzene*	115	114-445	190	4.6	178.08	9.17	209.4	6.2	33.8	7.3
Toluene*	117	116-329	220	4.6	178.15	6.64	63.8	4.5	14.1	3.1
Cumene[1]	129	130-303	195	5.5	177.13	7.33	107.5	5.0	21.5	3.9
Propylene carbonate*	158	153-371	269	5. 2	218.66	8.01	112.1	4.6	24.4	4.7
Diethyl phthalate	181	188-292	253‡	14.5 ‡	269.92	17.98	237.6	8.05	29.5	2.0‡
m-Toluidine	187	181-473	275	7.0	241.65	8.80	96.4	4.4	21.7	3.1
Glycerol*	190	183-413	324	14.5	291	18.3	189	7.7	24.5	1.7‡
Dimethyl phthalate	191	191-441	340	8.7	274.18	16.92	262	7.8	33.6	3.9
Triphenyl phosphite	200	202-361	260	13.0	296	25.0	414.3	10.2	40.6	3.1
α-Phenyl-o-cresol[1]	220	208-420	380	7.5	325.6	21.8	321.8	8.1	39.7	5.3
Salol	221	213-416	318	9.05	314.96	19.16	323.0	7.4	43.6	4.8
OTP	243	239-555	401	8.5	329.35	17.19	233.3	6.8	34.5	4.0
Sorbitol	268	263-420	384	26.3	369.16	30.35	163.4	n/a	n/a	n/a
Glucose	312	295-420	403	36.9	414	31.4	453.1	n/a	n/a	n/a
Cresol phthalein-dimethylether	312	308-499	480	16.4	383.2	27.9	489.5	9.3	52.6	3.2
Tri-α-naphtyl benzene	342	332-680	571	14.2	456.3	33.3	582.3	8.9	65.6	4.6
B_2O_3	530	533-1688	1031	30.5	723	22.0	455	3.65†	124.4†	4.1†

† Asymptotic behavior of H_x at $T>T_m$ is not well represented by λRT

[1] Alternate chemical name: cumene - isopropyl benzene; α-Phenyl-o-cresol - o-benzylphenol

II.5 Data Sensitivity

The sensitivity of the $\log a = B(1/\bar{H}_x - 1/\bar{H}_{x0})$ model to variation in the thermodynamic data will be explored using n-propanol as a typical material. Using the best available literature data we arrived at the fit shown in Fig. 3D with the value of B=79.1 kJ/mole as given in Table 1, where the details of the analysis can be found in the Supporting Information[58]. The values of the enthalpy of fusion and the liquid and crystalline heat capacities for n-propanol appear to be robustly determined, providing a solid point-of-departure for studying the effect of experimental error on the performance of the $1/\bar{H}_x$ mobility model. The effect of varying $\Delta\bar{H}_{fus}$ by ±10% is shown in Figs. 4A and B. Three potential sources of heat of fusion error are:

1. An error in the measured value of $\Delta\bar{H}_{fus}$ may be caused by impurities, although it is unlikely that a large amount of impurities would be missed.
2. A heat leak is more plausible source of error (especially in older calorimetry works) in which case the actual $\Delta\bar{H}_{fus}$ would be overestimated and the -10% case may be closer to the truth.
3. Another possible source $\Delta\bar{H}_{fus}$ error is variation in the enantiomer composition for molecules with a stereo-chemical center, which could result in either an overestimation or underestimation of $\Delta\bar{H}_{fus}$ (This also raises the possibility that mobility data were obtained for a sample with one mixture of enantiomers whereas the heat capacity data were obtained for another mixture).

4. If a glass forming material has multiple crystalline states the meaning of $\Delta\bar{H}_{fus}$ is unclear, where the $\Delta\bar{H}_{fus}$ used in the analysis may be either overestimated or underestimated.

Although these four sources of error are unlikely for the n-propanol data, they are the types of experimental error that should be considered. Examining the data in Figs. 4A and 4B, the key finding are: (i) The single parameter *B*, i.e. the slope of the line in Fig. 4A, is quite sensitive to presence of error in the heat of fusion and (ii) The residual plot shows that the size of the crossover region at high temperatures (or small values of $1/\bar{H}_x$) decreases if $\Delta\bar{H}_{fus}$ is made smaller by 10%.

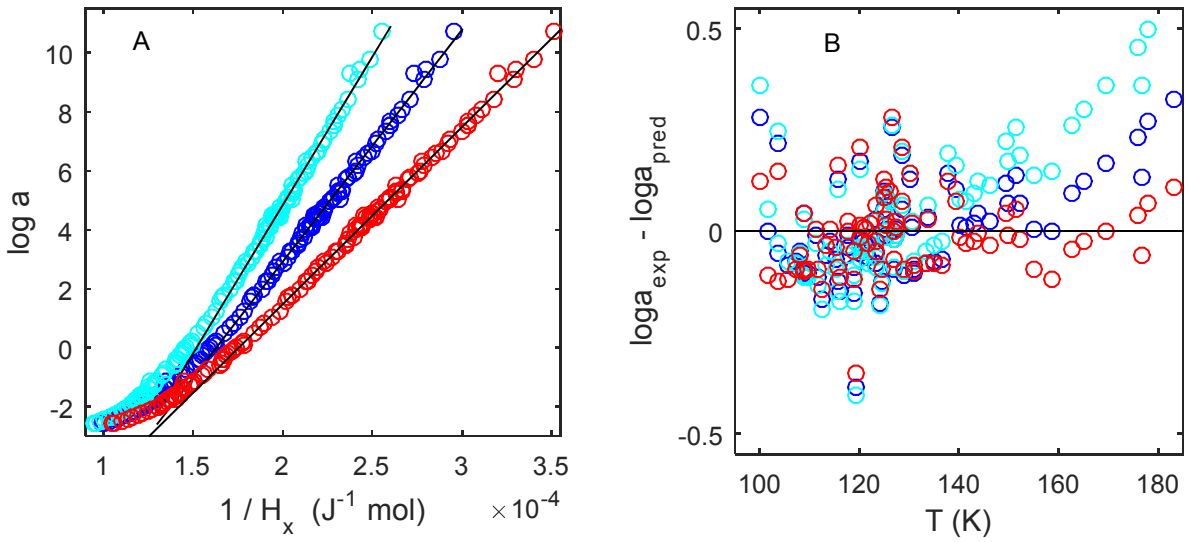

Figure 4 The effects of error in $\Delta\bar{H}_{fus}$ on the $1/\bar{H}_x$ mobility model and the model parameter *B*. (A) $\log a$ vs $1/\bar{H}_x$; blue – *B* = 79.1kJ/mol and ΔH_{fus}=5.4kJ/mol; cyan – B = 100.7kJ/mol and ΔH_{fus} =5.9kJ/mol; and, red – *B* = 60.1kJ/mol with ΔH_{fus}=4.9kJ/mol. (B) Residual analysis of data compared to $1/\bar{H}_x$ mobility model.

The effect of varying the super-cooled liquid heat capacity $\bar{C}_{p,liq}$ at T_g =98K for n-propanol by ±10% is examined in Fig. 5. When value of the liquid heat capacity at T_g is changed, the rest of the $\bar{C}_{p,liq}(T)$ curve in the super-cooled region has to be adjusted in order to recover the high temperature heat capacity as shown in Fig. 5A. The two cases considered in Fig. 5A correspond to the following hypothetical scenarios: (i) If a material has a tendency to partially crystallize in the super-cooled state, then the measured heat capacity, i.e. the green markers, may be lower than the true liquid heat capacity i.e. the solid green line. Partial crystallization is of more concern for adiabatic calorimetric measurement where the thermal equilibration times may be long. (ii) Data in the super-cooled state heat capacity may not be available, where a linear extrapolation of the liquid heat capacity above T_m is used i.e. the solid magenta line. Examining the data in Fig. 5B, unlike in case of the enthalpy of fusion, changes to the liquid heat capacity have a less dramatic effect on the slope of the $\log a$ vs $1/\bar{H}_x$ dependence, but it does cause a more rapid loss of linearity. Specifically, the magenta set in Fig. 5B is noticeably curved upward and the green set begins to turn into a sigmoidal curve.

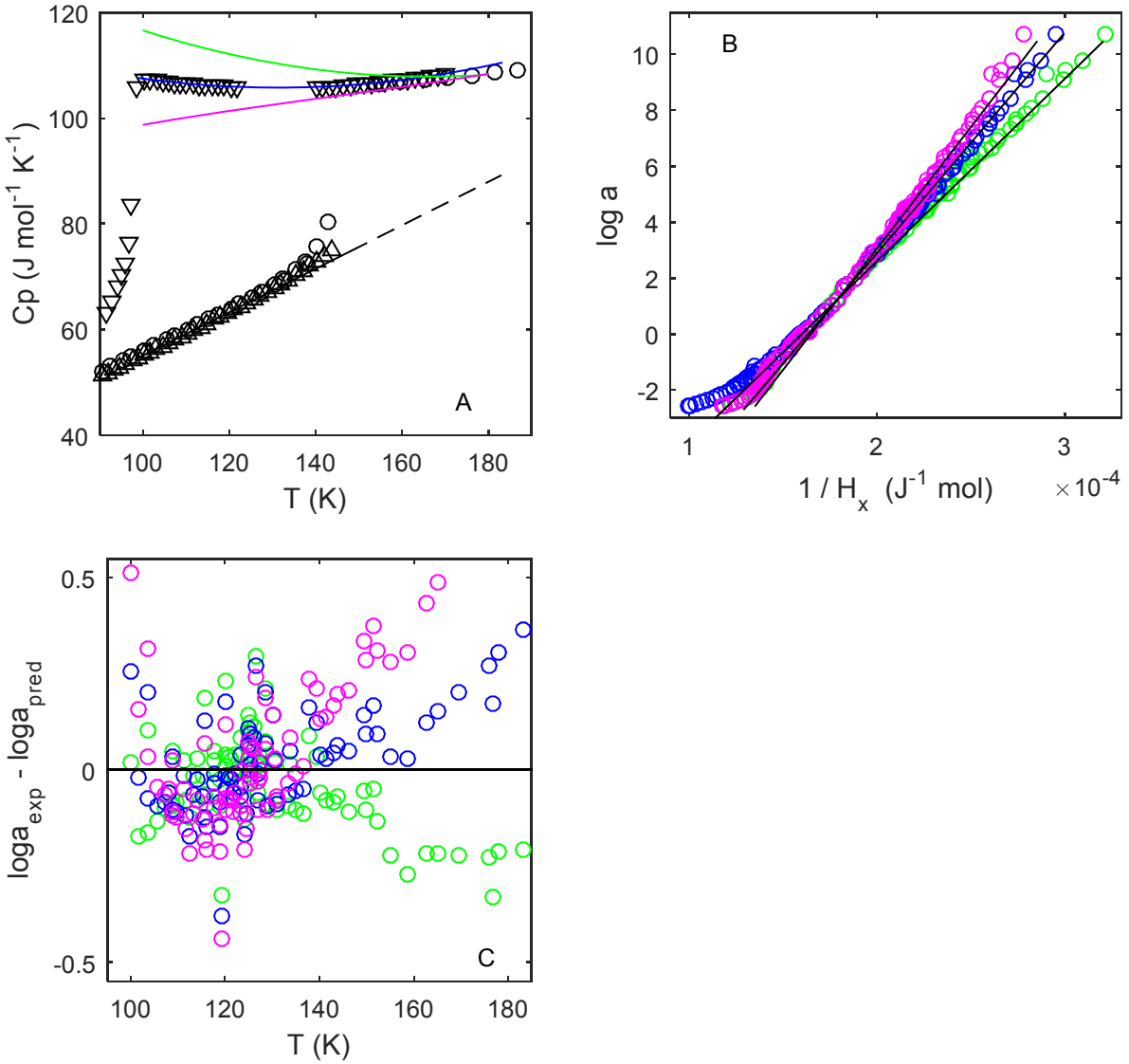

Figure 5 The effects of error in the liquid heat capacity on the $1/\bar{H}_x$ mobility model. (A) Variation in temperature dependence of liquid state heat capacity; heat capacity data (see Supporting Information[58] for references) – black markers, fit and extrapolation of crystalline heat capacity data – black solid and dashed lines, fit to liquid heat capacity used to obtain the value of B = 79.1kJ/mol shown in Table 1 – blue line, 10% increase in liquid heat capacity value at T_g – green line, 10% decrease in liquid heat capacity value at T_g – magenta line. (B) $\log a$ vs. $1/\bar{H}_x$ corresponding to blue, green, and magenta liquid heat capacity lines; the slope values are B = 79.1kJ/mol, B = 65.1kJ/mol, and B = 87kJ/mol, respectively; (C) Residual analysis of data compared to $1/\bar{H}_x$ mobility model.

The analysis in the previous two paragraphs shows that the functional form of the $\log a = B(1/\bar{H}_x - 1/\bar{H}_{x0})$ model is quite robust, where even with substantial changes in $\Delta\bar{H}_{fus}$ and $\bar{C}_{p,liq}(T_g)$ $\log a_T$ is still a nearly linear function of $1/\bar{H}_x$. However, changes in the experimental inputs used to determine the excess enthalpy have a strong effect on the value of the fitting parameter B and the range where $\log a$ vs $1/\bar{H}_x$ is linear as shown in Fig. 4A and 4B. Specifically, in Fig. 4B a value of $\Delta\bar{H}_{fus}$

that is 10% lower than the reported value (i.e. the red circles), result in the $\log a = B(1/\bar{H}_x - 1/\bar{H}_{x0})$ model fitting the mobility data for the entire T_g to T_A range from 98K to 183K for n-propanol thereby eliminating the crossover region. Similarly, a small modification of the super-cooled heat capacity such that the corresponding curve would lie between the blue and the green solid lines in Fig. 5A will also result in the $\log a = B(1/\bar{H}_x - 1/\bar{H}_{x0})$ model fitting the mobility data for the entire T_g to T_A range, where the residual would be located between blue and green circles in Fig. 5C. These variations are most probably outside the experimental uncertainty for n-propanol as reported in the original papers;[84,85] however, the analysis shows that accurate thermodynamic data is an essential requirement.

III. The Effect of Pressure on the Mobility

III.1 General Considerations

The analysis in Section II above shows that $\log a_T$ is proportional to $1/\bar{H}_x$. But, for data at p=1atm $1/\bar{U}_x$ is equally viable; specifically, $\bar{H}_x = \bar{U}_x + p\bar{V}_x$ where at atmospheric pressure the $p_a\bar{V}_x$ term is negligible. However, if the mobility is measured at elevated pressures the response predicted by $B(1/\bar{U}_x - 1/\bar{U}_{x0})$ will be different from that predicted by $B(1/\bar{H}_x - 1/\bar{H}_{x0})$, where $\bar{H}_{x0}$ and $\bar{U}_{x0}$ are respectively the enthalpy and internal energy in the reference state of $T = T_A$ and p=1atm.

The effects of pressure on entropy and enthalpy are evaluated using the standard thermodynamic relations:

$$\bar{S}(T,p) = \bar{S}(T,p_a) + \int_{p_a}^{p}\left(\frac{\partial \bar{S}}{\partial p'}\right)_T dp' = \bar{S}(T,p_a) + \int_{p_a}^{p}\left[-\left(\frac{\partial \bar{V}}{\partial T}\right)_p\right]dp' \tag{22}$$

$$\bar{H}(T,p) = \bar{H}(T,p_a) + \int_{p_a}^{p}\left(\frac{\partial \bar{H}}{\partial p'}\right)_T dp' = \bar{H}(T,p_a) + \int_{p_a}^{p}\left[-T\left(\frac{\partial \bar{V}}{\partial T}\right)_p + \bar{V}(T,p')\right]dp' \tag{23}$$

In Eqns. (22) and (23) the melting temperature, T_m, the entropy of fusion, $\Delta\bar{S}_{fus}$, and the enthalpy of fusion, $\Delta\bar{H}_{fus}$, are all functions of pressure. The relationship between these three quantities is given by the Clausius- Clapeyron equation

$$\frac{dT_m(p)}{dp} = T_m(p)\frac{\Delta\bar{V}_{fus}(p)}{\Delta\bar{H}_{fus}(p)} \tag{24}$$

where $\Delta\bar{V}_{fus}(p)$ is the change in molar volume upon melting. If the molar volumes in the crystalline and liquid states are known exactly, then Eqn. (24) contains no additional information as compared to Eqns. (22) through (23). However, if the $\bar{V}(T,p)$ function used in Eqns. (22-23) contains extrapolations (say, to pressure higher than the one at which the molar volume has been experimentally measured) and if the value of $T_m(p)$ has been independently measured, then Eqn. (24) provides a check of the validity of the extrapolations.

If $\bar{V} = \bar{V}(T,p)$ for both liquid and crystalline states is parameterized via the Tait equation[86] is given by

$$\bar{V}(T,p) = \bar{V}_a(T)\left[1 - c\ln\left(1 + \frac{p - p_a}{B_0 e^{-B_1 T}}\right)\right] \tag{25}$$

then the integrations in Eqns. (22-23) can be completed. Here c is the "universal" Tait constant with a value of 0.0894, B_0 and B_1 are material constants. The volume vs. temperature dependence at the atmospheric pressure is usually parameterized as exponential of a low order polynomial, i.e.

$$\bar{V}_a(T) = M V_0 \exp\left[a_1 (T - T_0) + a_2 (T - T_0)^2 + \ldots \right] \tag{26}$$

where M is the molar mass V_o is the specific volume in a reference state at T_o and 1 atm.

Using Eqns. (22) and (23) with the two $\log a(T, p)$ models give different predictions for the experimentally measured pressure dependence of the glass transition line. Specifically, since the glass transition line is the iso-$\log a$ line in the (T, p) space, its tangent is given by

$$\frac{dT_g}{dp} = -\left(\frac{\partial \log a}{\partial p} \right)_T \Bigg/ \left(\frac{\partial \log a}{\partial T} \right)_p \tag{27}$$

Thus, predictions of the $1/\bar{H}_x$, $1/\bar{U}_x$, and $1/T\bar{S}_x$ models evaluated at p = 1 atm are:

$$1/T\bar{S}_x: \qquad \frac{dT_g}{dp} = \frac{1}{\bar{C}_{px} + \bar{S}_x} T \left(\frac{\partial \bar{V}_x}{\partial T} \right)_p \tag{28a}$$

$$1/\bar{H}_x: \qquad \frac{dT_g}{dp} = \frac{1}{\bar{C}_{px}} \left[T \left(\frac{\partial \bar{V}_x}{\partial T} \right)_p - \bar{V}_x \right] \tag{28b}$$

$$1/\bar{U}_x: \qquad \frac{dT_g}{dp} = \frac{1}{\bar{C}_{px}} T \left(\frac{\partial \bar{V}_x}{\partial T} \right)_p \tag{28c}$$

where $\bar{C}_{px}$ is the molar excess constant pressure heat capacity evaluated at the temperature of interest. We will evaluate these three expression for the glass former OTP.

III.2 Ortho-terphenyl (OTP)

The mobility at elevated pressure has been measured for several materials.[87] However, OTP is the only material in the literature for which the pressure-volume-temperature (PVT) behavior in the crystalline state has been reported[31] and, hence, for which the analysis developed in the previous section can be carried out. In the same paper Naoki and Koeda also measured the PVT behavior in the liquid state; recently, the PVT behavior in liquid state was also measured by Casalini et al[88] for a wider pressure range. The data of Casalini et al are in good agreement with the data of Naoki and Koeda. The Tait equation parameterization of PVT data of Naoki and Koeda and of Casalini et al is given in the Table 2. The integrations in Eqns. (22) and (23) were performed to determine the entropy, enthalpy, and internal energy in the crystalline and liquid states; subsequently, the temperature and pressure dependence of the excess entropy, enthalpy, and internal energy were determined.

Table 2 Tait equation parameters for OTP (molar mass M=230.31 g/mol).

Data Source	T_0 (K)	V_0 (cm^3/g)	a_1 (1/K)	a_2 (1/K^2)	B_0 (MPa)	B_1 (1/K)
Liquid[88]	303.15	0.92870	7.266×10^{-4}	4.66×10^{-7}	888.4	5.17×10^{-3}
Liquid[31]	303.15	0.93084	7.136×10^{-4}	4.30×10^{-7}	622.5	4.39×10^{-3}
Crystal[31]	313.10	0.86103	2.493×10^{-4}	1.80×10^{-7}	912.3	2.91×10^{-3}

The pressure dependence of the mobility of OTP was experimentally determined via: photon correlation spectroscopy (PCS) by Fytas et al,[89] dielectric relaxation by Naoki et al,[90] specific heat spectroscopy by Leyser et al,[91] and viscosity measurements by Schug et al.[92] In Fig 6A two elevated pressure $\log a(T,p)$ isobars are given: at p=78.5MPa and at p=125MPa along with $\log a_T$ determined at p=1atm, i.e. 0.1MPa (which is a re-plotting of the data shown in Fig. 1A). The choice of p=125MPa is dictated by the fact that this is the highest pressure for which sufficient low and high temperature data is available, where Schug et al measured the viscosity at pressures up to 1GPa albeit for temperatures above T_A. Since Fytas et al, Naoki et al, and Schug et al reported their data at p=1atm as well as at elevated pressures, the isobars in Fig. 6A were constructed as follows: for each data set the p=1atm isobar was shifted vertically until it overlays with the rest of the $\log a_T$ data shown in Fig. 1A; then the same vertical shift was used for the elevated pressure isobars. As a result of this procedure it was found that the PCS and dielectric relaxation data agree well, whereas a certain mismatch exists between the spectroscopic and viscosity measurements (see Fig. 6A caption for details).

The prediction of the $1/\bar{H}_x$, $1/\bar{U}_x$, and $1/T\bar{S}_x$ models are shown in Fig. 6A, where B_{Ux}= B_{Hx} =233.3 kJ/mol, and B_{AG} = 96.0kJ/mol as determined from the p=1atm data as reported in Fig. 1. At p=1atm the $1/\bar{H}_x$ and $1/\bar{U}_x$ models coincide (and describe the super-Arrhenian $\log a_T$ well) whereas the $1/T\bar{S}_x$ model deviates from the data as has already been shown in Fig. 1D. However, at p=78.5MPa and especially p=125 MPa the three models predict a different response with the $1/\bar{U}_x$ providing the best fit and the $1/\bar{H}_x$ model the worst. Specifically, the $1/\bar{H}_x$ and $1/T\bar{S}_x$ models clearly miss the experimental data and the $1/\bar{U}_x$ model prediction is located between the spectroscopic data and viscosity data.

The $\log a(T,p)$ isotherms are shown in Fig. 6B, where the 268K and 275K isotherms are from specific heat spectroscopy[91] and the 303K isotherm from viscosity data.[92] Clearly, the slope of $\log a$ vs p as predicted by the $1/\bar{U}_x$ model is much closer to the data than that predicted using the $1/\bar{H}_x$ or $1/T\bar{S}_x$ models. It should be noted that the experimental isotherms for temperatures higher than 303K are available from Schug et al; however, these temperatures correspond to the cross-over region or even the above T_A region. The super-Arrhenian mobility models do not apply even at p=1atm above T_A; thus, it would be meaningless to consider the predicted pressure dependence at these higher temperatures. Notwithstanding this concern, the data and predictions shown in Fig. 6 demonstrate the superiority of the $1/\bar{U}_x$ model which captures quantitatively the super-Arrhenian temperature dependence at p=1atm and provides a reasonable description of the pressure dependence of the mobility for OTP. It is important to note that a better agreement with the data in Fig. 6 cannot be achieved by simply making the constant B in the $\log a = B(1/\bar{U}_x - 1/\bar{U}_{x0})$ model a function of pressure. Since the model predictions (i.e. solid lines in Fig. 6) lie between the spectroscopic data and the viscosity data, improving the fit to the former will inevitably cause worsening of the fit to the latter and vice versa. At this point we are not sure if the remaining discrepancies between the $1/\bar{U}_x$ model predictions and the data are caused by deficiency of the model or inconsistencies in the data.

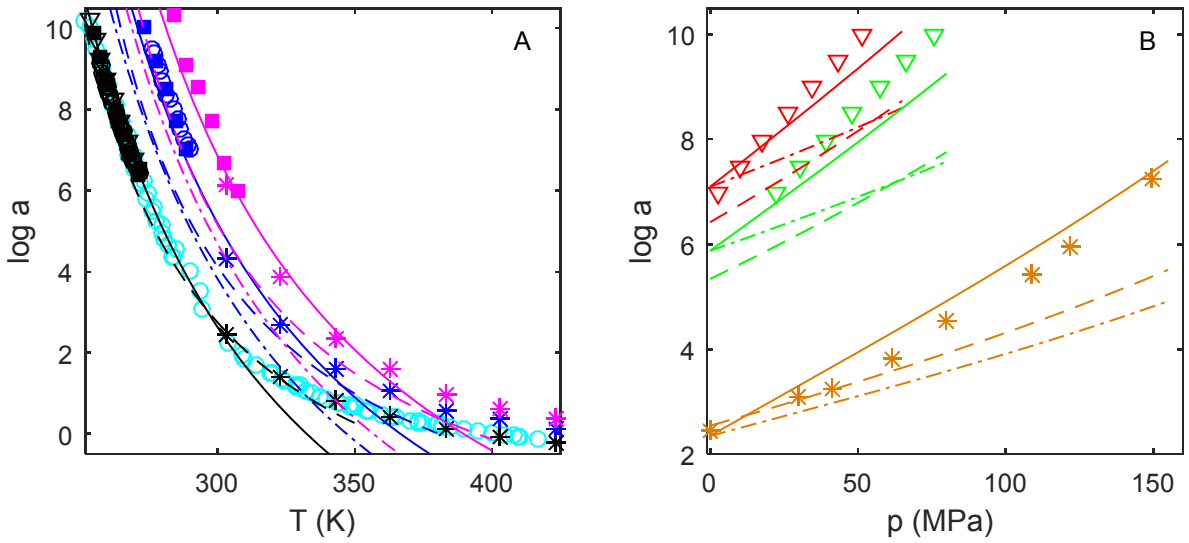

Figure 6. Effect of pressure on the $\log a$ mobility for OTP as described by the $1/\bar{H}_x$, $1/\bar{U}_x$, and $1/T\bar{S}_x$ models. Symbols: viscosity data of Schug et al[92] – stars,; PCS data of Fytas et al[89] – squares; dielectric relaxation data of Naoki et al[90] – circles; specific heat spectroscopy data of Leyser et al[91] – triangles. Lines: $1/\bar{U}_x$ model – solid, $1/\bar{H}_x$ model – dash-dotted, $1/T\bar{S}_x$ model (i.e. Adam and Gibbs) – dashed. (**A**) Temperature dependence of $\log a$ at 0.1MPa – black, 78.5MPa – blue, and 125MPa – magenta; $\log a_T$ at 0.1MPa from Fig 1A (reference) – cyan circles. (**B**) Pressure dependence of $\log a$ at 303K – orange, 275K – green, 268K – red.

Pressure dependence of mobility at a lower temperature is addressed by determining how the value of T_g changes with pressure, where $T_g(T,p)$ line is iso-mobility (i.e. constant $\log a$) line. The predictions for various models are given in Eqn. (28). Experimentally the pressure dependence of T_g for OTP was determined by Atake and Angell[93] using the DSC measurements. The results are summarized in the Table 3. The $1/\bar{H}_x$ and $1/T\bar{S}_x$ models under-predict the experimental value, where the $1/\bar{U}_x$ model is closer to the experimental dT_g/dp data, although the agreement is not quantitative. Although Atake and Angell did not provide an error estimate for their dT_g/dp value, the error could be significant for two reasons: first, the $T_g(p)$ value was found to be dependent on the experimental protocol i.e. pressurizing in the liquid state and then vitrifying vs the reversing the temperature-pressure history; and second, the experimental $T_g(p)$ dependence is clearly curved in case of OTP so that the value given in the Table is based on only two data points. If more experimental points are included in the analysis, we determined that at p=0 the experimental dT_g/dp is 0.22, which is quite close to the 0.20 predicted by the $1/\bar{U}_x$ model.

Table 3. Comparison of pressure dependence of Tg for the three mobility models with experimental data.

	Experimental [93]	$\frac{1}{T\bar{S}_x}$	$\frac{1}{\bar{H}_x}$	$\frac{1}{\bar{U}_x}$
$\left.\frac{dT_g}{dP}\right\|_{p\to 0}$ (K/ *MPa*)	0.26	0.17	0.11	0.20

IV. Discussion

A new model for describing the super-Arrhenian $\log a(T,p)$ mobility for glass forming liquids has been developed; specifically, $\log a = B(1/\bar{U}_x - 1/\bar{U}_{x0})$, where $\bar{U}_x$ is the excess internal energy that is independently determined from calorimetric data for the liquid and crystal, $\bar{U}_{xo}$ is the excess internal energy in a reference state and B is a material constant. This single material parameter mobility model quantitatively relates the super-Arrhenian mobility to the thermodynamic state (really the thermostatic state) of the material. The $1/\bar{U}_x$ model accurately described the data for 21 glass forming materials, which we believe are all of the molecules where there is sufficient mobility and thermodynamic data to critically evaluate the $1/\bar{U}_x$ model. The $1/\bar{U}_x$ model provides a connection between the super-Arrhenian mobility and the equilibrium thermodynamic state.

A key feature of the analysis is that it only focused on mobility in the equilibrium (more precisely super-cooled) region and does not employ significant extrapolations of thermodynamic data. For several materials listed in Table 1 no extrapolation of the heat capacity data was required in the temperature range that was used to validate the $1/\bar{U}_x$ model. And for temperatures above T_m where extrapolation of the crystalline heat capacity was required, for most materials a benign linear extrapolation was used. Moreover, the high temperature extrapolations of the crystalline data only affects the cross-over portion and the Arrhenian portion of the curve, which is not what the $1/\bar{U}_x$ model is designed to describe. This is in contrast to much of the literature analysis of mobility based on the Adam-Gibbs (AG) model, where the treatment often depends critically on the assumption that the excess (or configurational) entropy vanishes at a finite temperature T_2 as given in Eqn. (5) –a condition that is experimental inaccessible. Thus, the results shown in this paper are just the straightforward integration of experimental thermodynamic data, where there are no implicit assumptions or large extrapolations of the experimental data. The fact that the $1/\bar{U}_x$ model is able to describe mobility changes of ten or more orders-of-magnitude using just the experimental data without massaging the data and/or significant extrapolation provides strong evidence that the $1/\bar{U}_x$ model captures the essential physics of the super-Arrhenian behavior of glass forming liquids.

The $1/\bar{U}_x$ model has a number of features that are essential for any physically based model. *First*, $\log a$ is not a linear function of $1/\bar{U}_x$ at high temperatures, where at temperatures above T_A the material exhibits Arrhenian behavior. Also, the equilibrium $1/\bar{U}_x$ model fails when the material falls out of equilibrium below T_g as illustrated by the case of α-phenyl-o-cresol given in the Supporting Information[58]. Thus, the model fails outside of the super-Arrhenian region – if a $\log a$ model were to describe the two regions presumably controlled by different physics, it would either be truly profound or more likely just a curve fit. *Second*, the $1/\bar{U}_x$ model has only one parameter B that is robustly determined from the $\log a_T$ vs $1/\bar{U}_x$ plot. This is in contrast to most of the $\log a_T$ models that have two or more fitting parameters that are often correlated. The AG model has a single fitting parameter, but even here analysis with AG typically employs T_2 as a second fitting parameter (see Introduction). A small number of parameters (ideally one) that are robustly determined from the data is an important feature of a physically based model. *Third*, during the course of this analysis materials were examined that did not result in a linear relationship between $\log a_T$ and $1/\bar{U}_x$, where there were issues with the experimental data. Specifically, for toluene, ethyl benzene, and glycerol it is difficult to avoid crystallization in the super-cooled state; propylene carbonate has other experimental problems as discussed in more details in the Supporting

Information[58] – where for all of these materials the range where $\log a_T$ vs $1/\bar{U}_x$ plot was linear was smaller and the crossover range between super-Arrhenian and Arrhenian regimes was larger. It is reassuring that the model is unable to fit data where the fundamental assumptions of the model are violated.

Polymers are an important class of glass forming materials that were not included in this analysis. Many polymers can be readily super-cooled and there is excellent mobility data from a variety of experimental techniques. Measurement of the heat capacity for the liquid, super-cooled liquid and glassy states is a standard measurement in many laboratories. The challenge is in measuring the crystalline heat capacity and, most importantly, the heat of fusion. The difficulty is in producing crystalline polymers without defects, where chain ends and slow crystalline kinetics conspire to make production of defect free polymer crystals nearly impossible. Even the unavoidable presence of chain ends can affect the experimentally measured heat of fusion, which is typically the most important contribution to the determination of $\bar{H}_x$, and hence $\bar{U}_x$. Finally, even if the challenges listed above can be overcome for some polymers, the question remains how to proceed with regard to polymeric systems for which the crystalline state does not exist such as atactic polymers, random co-polymers, etc. There are three potential approaches to incorporate polymers in the analysis: (i) Use a sequence of dimer, trimer, tetramer, etc. oligomers to arrive at the extrapolated value of $\Delta\bar{H}_{fus}$ for polymers. This approach has been successfully realized for alkenes;[94,95] as a result, the $\Delta\bar{H}_{fus}$ value for LDPE is well established.[52] As mentioned in Section II.1, the problem in case of LDPE is lack of mobility data of sufficient range rather than thermodynamic data. (ii) Use molecular simulations to construct defect free unit cells. (iii) Allow $\Delta\bar{H}_{fus}$ to be a fitting parameter, although this approach is less satisfying as it results in a two parameter model. These approaches are potential avenues for future research.

The $1/\bar{U}_x$ super-Arrhenian mobility model has obvious similarities to the well-known Adam-Gibbs (AG) $1/T\bar{S}_x$ model, but there are important differences – the most significant being the ability of the $1/\bar{U}_x$ model to linearize the super-Arrhenian $\log a_T$ mobility data for 10 or more orders-of-magnitude. The AG derivation was spurred by a desire to reconcile the $\log a_T$ singularity at $T = T_{VTF}$ in the VTF/WLF mobility relationship with the Kauzmann paradox,[96] where a critical part of the theory is that the linear extrapolation of the configurational entropy measured above T_g goes to zero at a finite temperature below T_g. An important feature of the AG model is that it proposes a specific molecular mechanism for the origin of the super-Arrhenian behavior observed in glass forming liquids; specifically, (i) that the molecular mobility is a thermally activated process where the activation energy depends upon the size of a cooperatively rearranging region and (ii) there is a lower limit to the size of the cooperatively rearranging region, since it must have at least two available configurations. The AG model employed the configuration entropy defined as the liquid minus the glassy entropy, where the excess entropy represents the same idea but does not suffer from the thermal-pressure history dependence associated with defining unique entropy for the glassy state. In contrast, the $\log a$ vs $1/\bar{U}_x$ linear relationship developed in this paper does not depend upon postulating a specific molecular mechanism – thus, it must be evaluated by its ability to predict the $\log a$ mobility data, where it is superior to the AG model as shown in Figs 1 through 3 and in the Supporting Information[58]. Even though the results of this paper demonstrate that $1/\bar{U}_x$ is a significantly better description of the mobility in the super-Arrhenian region of glass forming liquids than $1/T\bar{S}_x$, it is important to remember the postulate that the mobility is controlled by configurational/excess thermodynamic quantities was originated by Gibbs and DiMarizo[29] and quantified by Adam and Gibbs.[32]

In the density scaling model of glass forming liquids, the temperature and pressure dependence of $\log a$ is described as $\log a = f\left(T^{-1}V^{-\gamma}\right)$, where (i) the function f and parameter γ are material specific and (ii) the volume dependence on temperature and pressure is given by experimentally determined equation-of-state. The density scaling approach has been discussed in several reviews.[87,97] This density scaling postulate is not in conflict with the $1/\overline{U}_x$ equation reported here, where if both are true then the implication is that the excess internal energy is also a function of the same quantity $\overline{U}_x = g\left(TV^{\gamma}\right)$. This is an important connection that should be explored further.

Recently is has been experimentally observed for several small molecule glass formers that the mobility decreases (i.e. $\log a$ increases) when a strong electric field is applied isothermally at temperatures slightly above the conventional T_g.[42,43] A key question is: can models for describing mobility of glass forming materials predict the effect of the static electric field? Assuming that the mobility is given by the $B/\overline{U}_x$ model, the change in mobility upon application of an electric field is

$$\Delta_E \log a = B\left(\frac{1}{\overline{U}_x(E)} - \frac{1}{\overline{U}_x(0)}\right) \tag{29}$$

Alternatively, if one assumes that the mobility is given by the $\overline{B}_{AG}/T\overline{S}_x$ then the predicted change in mobility upon application of an electric field, *E*, is given by

$$\Delta_E \log a = B_{AG}\left(\frac{1}{T\overline{S}_x(E)} - \frac{1}{T\overline{S}_x(0)}\right) \tag{30}$$

The derivation of the expressions for the energy and entropy of a dielectric material in the presence of electric field follows standard thermodynamics,[98] where the results are:

$$\overline{S}(E) = \overline{S}(0) + \frac{1}{2}\overline{V}\varepsilon_o\left(\frac{\partial\varepsilon}{\partial T}\right)_{E,p}E^2 \tag{31}$$

and

$$\overline{U}(E) = \overline{U}(0) + \frac{1}{2}\overline{V}\varepsilon_o\left[T\left(\frac{\partial\varepsilon}{\partial T}\right)_{E,p} + \varepsilon\right]E^2 \tag{32}$$

where ε is the dielectric constant of the material ε_o is the permittivity of vacuum and $\overline{V}$ is the molar volume. The excess quantities in Eqns. (29) and (30) are obtained by subtracting crystalline values from the liquid values calculated using Eqn. (32) and (31), respectively.

For most materials (i) the sign of the derivative $\partial\varepsilon/\partial T$ is negative and (ii) the absolute value $\partial\varepsilon/\partial T$ for liquid is vastly greater than that for crystal; thus, Eqn. (31) predicts that the entropy is lowered upon application of electric field. Thus, according to the AG model it follows from Eqn. (30) that $\Delta_E \log a$ is positive, which qualitatively agrees with experimental observations. The problem, however, is that according to Richert[43] this increase in $\log a$ is significantly over-predicted by the AG model – in case of the small molecule glass former CPDE by at least a factor of 4. Now examining the expression (32), the effect of electric field on the internal energy is less pronounced than on the entropy, since the $T\,\partial\varepsilon/\partial T$ term (which is negative) is counterbalanced by the ε term (which is positive) in the square brackets in Eqn. (32). This suggests that the internal energy model will be in better agreement with the data. Using the data of Samanta and Richert,[42] the predictions of both the $1/T\overline{S}_x$ and $1/\overline{U}_x$ models given via Eqns. (29) and (30) are compared vs experimental data in Table 4. The predictions of the $1/\overline{U}_x$ model present an improvement as compared to the $1/T\overline{S}_x$ model, although agreement with the experiment is not quantitative. The negative prediction $\Delta_E \log a$ for propylene carbonate is a result of the very large value of ε_x. One

should note that the electrical field experiments are challenging, where the experimentally $\Delta_E \log a$ measured shift upon application of a very large 500kV/cm field is equivalent to that caused by a fraction of a degree change in temperature. Thus, the modest agreement of the $\log a \sim 1/\bar{U}_x$ is satisfying, considering the difficulty of these experiments.

Table 4. Comparison of the effect of static electric field on mobility predicted by the $1/T\bar{S}_x$ and $1/\bar{U}_x$ models with experiments for several small molecule glass formers.

Material	T (K)[a]	E[a] (kV/cm)	$\bar{V}$[a] (cm^3/mol)	ε_x[a]	$\frac{\partial \varepsilon_x}{\partial T}$[a] (1/K)	$\bar{B}_{AG}$ (kJ/mol)	$\Delta_E \log a \times 100$		
							Exp.[a]	$\frac{\bar{B}_{AG}}{T\bar{S}_x}$[b] model	$\frac{\bar{B}}{\bar{U}_x}$[b] model
Propylene carbonate	168	360	75.7	94	-0.50	43.2[b] (44.9)[a]	3.5	13	-1.8
Glycerol	216.8	225	72.0	62	-0.41	(67.4)[a]	1.0	n/a[c]	0.6
Salol	234	450	171.3	5.3	-0.044	107.5[b] (112.8)[a]	1.4	2.5	1.6
CPDE	335	217	293.8	15	-0.073	243.8[b] (174)[a]	0.3	1.1	0.6

a – Values from Samanta and Richert, where $\varepsilon_x = \varepsilon_{liq} - \varepsilon_{cryst}$ is difference in the dielectric constant of liquid and crystal.

b – This work

c – The Adam-Gibbs model parameter for Glycerol could not be robustly determined because the $\log a_T$ vs $1/T\bar{S}_x$ dependence is curved (see Supporting Information[58] for details).

It is well established that free surfaces that occur in nanopores or thin films can dramatically depress the T_g of glass formers. However, both the $1/T\bar{S}_x$ and $1/\bar{U}_x$ models apparently predict the opposite behavior; specifically, consider a small cluster of molecules, where in the limit of just one molecule the difference between the "liquid" and the "crystalline" states vanishes, causing the excess quantity (i.e. liquid minus crystalline) to go to zero and thus causing $\log a$ going to infinity. This absurd result does not invalidate the excess quantities based models. Rather it shows that the an excess quantity based mobility mechanism (like that in the $1/T\bar{S}_x$ or $1/\bar{U}_x$ models) is for strictly bulk phenomenon, whereas if additional mobility/relaxation mechanisms becomes available due to presence of surfaces, then that new mechanism may control the system's mobility behavior.

The $\log a = B(1/\bar{U}_x - 1/\bar{U}_{x0})$ model has one material dependent property. It is of interest to see if B is correlated with some thermodynamic or structural feature of the 21 molecules in Table 1 for which values of B were determined. A number of quantities were examined, where a correlation of B with the heat of fusion is shown in Fig. 7A. The trend line in Fig. 7A passes through the origin and has a slope of C=16

$$B \approx C\,\Delta\bar{H}_{fus} \tag{33}$$

The modest scatter in Fig. 7A is remarkable considering that the experimental data leading to this correlation occurs via nearly 140 research publications that span nearly a century, where for a number of materials the research group(s) measuring the mobility was different than the research group(s) that measured the thermodynamic properties. The worst outlier in Fig. 7A is sorbitol – a material for which

we have concerns about the liquid heat capacity data (see Supporting Information[58] for details). Of the 21 molecules reported in Table 1 and Fig. 3 sorbitol and glucose have stereo-chemical centers that result in enantiomers. In the papers from which the thermodynamic and mobility data were taken for these two materials, there was no mention of any special care being taken to ensure enantiomeric or isomeric purity of the materials or of even characterization of the relative amount of each of the enantiomers. It is of considerable interest to expand the material set, especially the need to determine if polymers follow the same "universal" (i.e. with the same value for the constant C) behavior predicted by Eqn. (33), where this will require additional experimental or simulation data. The correlation expressed by Eqn. (33) does not mean that the equation for $\log a$ actually contains $\Delta\bar{H}_{fus}$ in the numerator instead of B. If this were the case the parameter B would possess a very specific dependence on pressure since $\Delta\bar{H}_{fus} = \Delta\bar{H}_{fus}(p)$, where for OTP this additional pressure dependence would worsen the fit to the higher pressure isobars. Thus, the correlation of the parameter B with $\Delta\bar{H}_{fus}$ is interesting, but a clear physical connection has not been established.

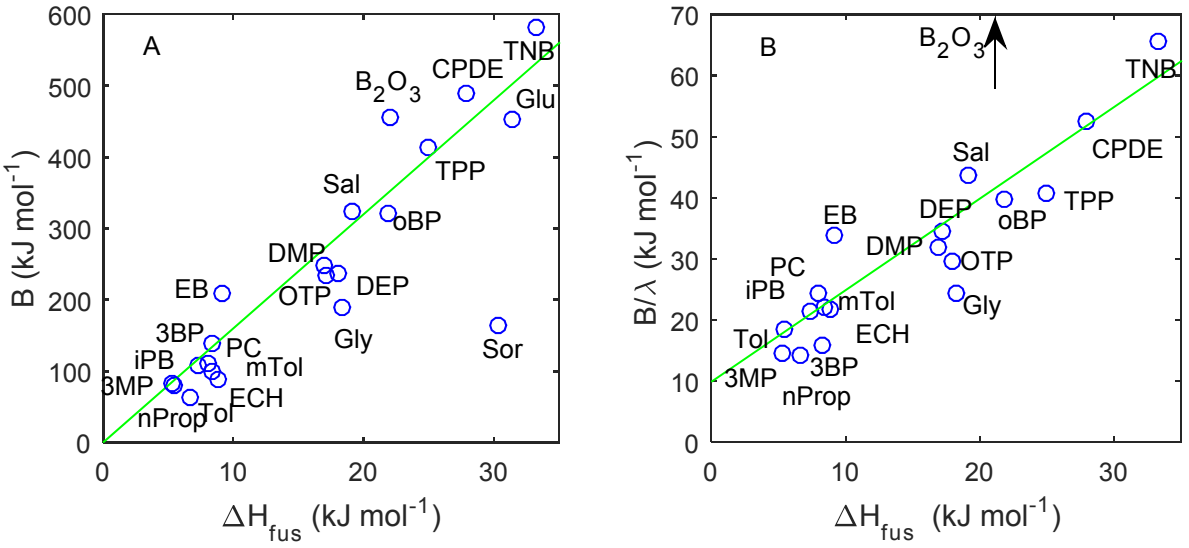

Figure 7. (A) Correlation of B with ΔH_{fus} for glass forming liquids. Designation of materials is given in caption for Fig. 3. Solid green is trend line with a slope of 16. (B) Same correlation for the quantity B/λ. Note that only the materials for which λ could be robustly determined are present (see Table 1 and Supporting Information[58] for details), where the trend line has the slope of 1.5 and the intercept value is 10 *kJ/mol*. The value for B_2O_3 in Fig. 7B is 124.4.

What type of process could lead to $\log a \sim 1/\bar{U}_x$ mobility relationship? Clearly the standard Transition State Theory (TST) cannot be the mechanism since RT is in the denominator in TST rather than $\bar{U}_x$ is in the new $\log a$ model. Alternatively, in the Adam-Gibbs (AG) model[32] it was assumed that TST was operative, but the barrier height for the transition was proportional to the number n of molecular units participating in the transition (i.e. size of the cooperatively re-arranging region, CRR), which was assumed to be a function of temperature. Thus, in the AG model the mobility is given by

$$\log a_T = \frac{n(T)\Delta E}{RT} \tag{34}$$

where ΔE is the intrinsic potential barrier for a single molecular unit. The postulate in the AG model was that a minimum number of configurations must exist in a CRR for a relaxation to occur. If the number of configurations per unit volume decrease (as given by the molar configurational/excess entropy) then the

size of CRR had to proportionally increase; thus, $n\bar{S}_x = \text{Const}$ which then results in the AG model given in Eqn. (4). As the temperature is decreased with an associated decrease in the excess entropy, the AG model predicts that the size of the CRR increases. Alternatively, one could postulate that there is a minimum amount of internal energy in a CCR needed for relaxation, where if the molar excess internal energy decreases there must be a proportional increase in the number of units in the CCR. This postulate results in

$$n(T) = \frac{\bar{U}_x^{\infty}}{\bar{U}_x(T)} \tag{35}$$

where $\bar{U}_x^{\infty}$ is the maximum possible molar excess internal energy reached at high temperatures. Combining Eqns. (34) and (35), the resulting expression for $\log a$ would have an extra T in the denominator as compared to $1/\bar{U}_x$ mobility model that has successfully described the super-Arrhenian mobility as reported in this paper. The key issue in the AG approach (or a similar form using the excess internal energy) is that the size of the CRR dramatically increases with decreasing temperature, where the temperature dependence of *n(T)* is the origin of the super-Arrhenian behavior in glass forming liquids. The existence of the length scale (static or dynamic) that increases with decreasing temperature which can be associated with the CRR of the AG theory is still a subject of debate with both experimental and computational research (see discussion in the review by Berthier and Biroli[99] and references therein).

The form of $\log a \sim B/\bar{U}_x$ mobility model is quite suggestive. Specifically, the fact that the temperature dependence of the relaxation time is the exponential of a rather benign function of temperature (i.e. $\bar{U}_x(T)$ as illustrated by Figs. 1C and 2C) hints at some connection with the TST. In the derivation of the TST expression,[100] the main result is that the time for going over a potential barrier (which could be the Gibbs free energy, the potential energy, etc.) under the influence of random pushes is given by

$$\frac{\tau}{\tau_0} \sim \exp\left(\frac{\Delta E}{D}\right) \tag{36}$$

where D is the intensity of the pushes or if the system in question is a Brownian particle – the diffusivity. The exponential in Eqn. (36) is a consequence of the stationary distribution having the form

$$p_s(z) \sim \exp\left[-\frac{E(z)}{D}\right] \tag{37}$$

where z is the reaction coordinate along which the transition is taking place. When the Gibbs theorem[101] for a system in a thermostat is invoked, the stationary distribution becomes the canonical/Boltzmann distribution and $D = RT$ (where T is the thermodynamic temperature) and the standard TST expression emerges. The above reasoning applies for a system in equilibrium; however, in the case of a metastable state (where the true equilibrium is the crystalline state) more than one quantity with the meaning of "temperature" may be usefully defined, where such a second temperature, say T_x, would be different from the thermodynamic temperature T. For example one can speculate that the process responsible for the slow dynamics in the super-cooled state is described by the TST like expression, where the "diffusivity" is given as $D = RT_x$, where in turn T_x is related to the excess internal energy $\bar{U}_x$.

How can a "second temperature" related to $\bar{U}_x$ be defined? Consider the asymptotic behavior of the excess enthalpy for OTP at temperatures above the melting point as shown by the red line in Fig. 8, where the melting temperature is where the $\bar{H}_x$ (i.e. black line) and the $T\bar{S}_x$ (i.e. blue line) intersect. Remember that for p = 1atm (which is condition where heat capacity data are available) $\bar{H}_x$ is essentially the same as $\bar{U}_x$. Somewhat surprisingly the data shows that this asymptote passes through the origin. Thus,

$$\bar{H}_x(T) \approx \lambda RT \qquad T > T_m \tag{38}$$

where λ is a dimensionless factor. This behavior is observed for most of the materials listed in Table 1, where yet again the materials that do not follow the pattern are the ones for which the heat capacity data are the least certain. The slope of the asymptote, i.e. λR, is approximately the entropy of fusion $\Delta\bar{S}_{fus}$. The values of λ are given in Table 1, where the asymptotes used to determine them are shown in the Supporting Information[58] and Figs. 2C and 8 for each of the 21 materials. The physical meaning of the behavior implied by Eqn. (38) is straightforward. The derivative of Eqn. (38) is

$$\left(\frac{\partial \bar{H}_x}{\partial T}\right)_p = C_{p,liq}(T) - C_{p,cryst}(T) = \lambda R \qquad T > T_m \tag{39}$$

It follows that the crystalline heat capacity extrapolated to high temperatures is parallel to the liquid heat capacity, where the difference between the liquid and crystalline excess heat capacity is roughly the increase in the entropy that occurs when the crystal melts. From a classical perspective each degree of freedom that is released upon melting carries a $R/2$ contribution to the heat capacity; thus, 2λ is the number of degrees of freedom in the liquid that were not present in the crystalline state. We will now define a second "temperature" $T_x(T)$ as

$$T_x(T) \equiv \frac{1}{\lambda R}\bar{H}_x(T) \tag{40}$$

An intriguing observation shown in Fig. 8 for OTP (and in the Supporting Information[58] for the other materials) is that the asymptotic behavior begins at approximately T_A. This means that the temperature T_x is a mapping of the standard thermodynamic temperature T such that it coincides with T at $T \geq T_A$, but T_x becomes progressively *smaller* than T at $T < T_A$ which can be seen in Fig. 8 as the difference between the red and the black lines. Finally we rewrite the mobility equation (8) as

$$\log a_T = \frac{B}{\lambda}\left[\frac{1}{RT_x(T)} - \frac{1}{RT_x(T_0)}\right] \tag{41}$$

Eqn. (41) has the form of the standard TST expression albeit with the temperature T_x. From this perspective the explanation for glassy behavior is that only the portion RT_x of the overall RT "thermal energy" is relevant for the rate limiting relaxation process that controls the super-Arrhenian behavior. Having a process controlled by T_x vs T is what makes it possible for some materials to exhibit the glass transition at a high thermodynamic temperature, since the temperature that matters is T_x, not T, and it can be significantly smaller as seen in Fig. 8.

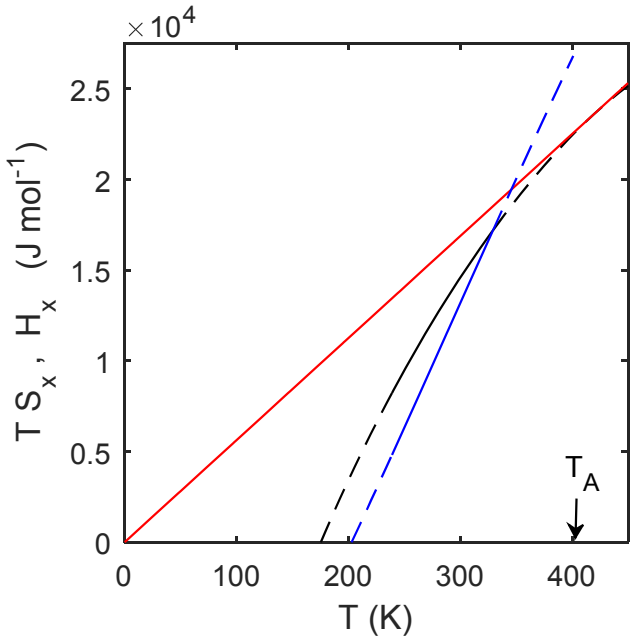

Figure 8 Asymptotic behavior of $\bar{H}_x$ at high temperature for OTP. $T\bar{S}_x$ – blue; $\bar{H}_x$ (or equivalently $\bar{U}_x$ at p=1atm) – black; asymptotic line – red. Experimental $\bar{H}_x$ and $T\bar{S}_x$ data from Chang and Bestul[65]

When using T_x, the quantity B/λ is the activation barrier, where the values are given in Table 1 for the 19 out of 21 glass forming materials for which it could be estimated (see Supporting Information[58] for details). The activation energy B/λ is correlated with the enthalpy of fusion as shown in Fig. 7B, where the quality of correlation is comparable to that displayed in Fig. 7A. There is one dramatic exception – B_2O_3; this is the only oxide on the list of glass formers in Table 1. It would be of great interest to have more oxide examples to observe if they form a different trend line. Unlike in case of the B parameter itself, the trend line for B/λ vs $\Delta\bar{H}_{fus}$ does not pass through the origin. Comparing the values of the activation barriers of the mechanisms operational below T_A, i.e. B/λ, and above T_A, i.e. $\bar{E}_A$, this ratio is between 2 and 7 for 19 materials listed in Table 1. It is tempting to interpret the ratio of these barriers as the estimate of how many molecular units participate in the mechanism responsible for low temperature, super-Arrhenian behavior assuming that the high temperature Arrhenian liquid behavior is unimolecular. Thus, the number of molecular units is close to that in the CRR of the AG model (i.e. 4 to 8 at T_g). However, there is a critical difference between the current model and the AG model. The AG explanation of the dramatic increase in $\log a$ is the increase in the size of the CCR; on the other hand, in the super-Arrhenian mobility mechanism contained Eqn. (41) it is the departure of the second temperature T_x from the thermodynamic temperature T that drives the super-Arrhenian increase in $\log a$, where the number of molecular units participating in the transition remains constant.

In this paper it has been demonstrated that the super-Arrhenian behavior, which is the key signature of glass forming materials, is quantitatively described by $\log a = B[1/\bar{U}_x - 1/\bar{U}_{x0}]$, where the single material dependent parameter B was correlated with the heat of fusion. The $1/\bar{U}_x$ mobility model is a robust description of the super-Arrhenian behavior of glass forming liquids that has been demonstrated for all materials for which there is sufficient mobility and thermodynamic data for critical evaluation. It has also been shown that the $1/\bar{U}_x$ mobility model has a structure consistent with transition state theory, but with a 'second temperature' T_x that is equal to the thermodynamic temperature T above T_A, but that

becomes significantly less than T as the temperature is decreased. Based upon this new perspective on the super-Arrhenian behavior of glass forming liquids there are several questions that need to be answered: What molecular processes are contained in $\overline{U}_x$? Why do the processes contained in $\overline{U}_x$ control the super-Arrhenian mobility? What happens at T_A such that the process controlling the mobility changes from being activated by T to T_x? Why is the activation energy in the super-Arrhenian region below T_A two to seven times greater than the Arrhenian activation energy above T_A? These questions will be the subject of future research, where determination of the molecular mechanism behind the $1/\overline{U}_x$ model is the next challenge.

Acknowledgements
This work was supported by National Science Foundation Grant Number 1363326-CMMI.

References

[1] E. N. d. C. Andrade, Nature (London) **125**, 309 (1930).
[2] E. Thoms, A. Grzybowski, S. Pawlus, and M. Paluch, J. Phys. Chem. Lett. **9**, 1783 (2018).
[3] L. A. Utracki, J. Macromol. Sci. B **10**, 477 (1974).
[4] H. Z. Cummins, G. Li, Y. H. Hwang, G. Q. Shen, W. M. Du, J. Hernandez, and N. J. Tao, Z. Phys. **B 103**, 501 (1997).
[5] I. Avramov, J. Non-Cryst. Solids **351**, 3163 (2005).
[6] H. Vogel, Phys. Z. **22**, 645 (1921).
[7] G. S. Fulcher, J. Am. Ceram. Soc. **8**, 339 (1925).
[8] G. Tammann, J. Soc. Glass Tech. **9**, 166 (1925).
[9] M. L. Williams, R. F. Landel, and J. D. Ferry, J. Am. Chem. Soc. **77**, 3701 (1955).
[10] T. Hecksher, A. I. Nielsen, N. B. Olsen, and J. C. Dyre, Nat. Phys. **4**, 737 (2008).
[11] G. B. McKenna and J. Zhao, J. Non-Cryst. Solids **407**, 3 (2015).
[12] F. Stickel, E. W. Fischer, and R. Richert, J. Chem. Phys. **102**, 6251 (1995).
[13] M. Paluch, J. Gapinski, A. Patkowski, and E. W. Fischer, J. Chem. Phys. **114**, 8048 (2001).
[14] S. C. Waterton, J. Soc. Glass Tech. **16**, 244 (1932).
[15] J. C. Mauro, Y. Yue, A. J. Ellison, P. K. Gupta, and D. C. Allan, Proc. Natl. Acad. Sci. U.S.A. **106**, 19780 (2009).
[16] I. Avramov and A. Milchev, J. Non·Cryst. Solids **104**, 253 (1988).
[17] Y. C. Elmatad, D. Chandler, and J. P. Garrahan, J. Phys. Chem. B **113**, 5563 (2009).
[18] M. H. Cohen and G. S. Grest, Phys. Rev. B **20**, 1077 (1979).
[19] D. Kivelson, S. A. Kivelson, X. Zhao, Z. Nussinov, and G. Tarjus, Physica A **219**, 27 (1995).
[20] B. Schmidtke, N. Petzold, R. Kahlau, and E. A. Rossler, J. Chem. Phys. **139**, 084504 (2013).
[21] H.-N. Lee, K. Paeng, S. F. Swallen, and M. D. Ediger, Science **323**, 231 (2009).
[22] C. F. Popelar and K. M. Liechti, J. Eng. Mater.-T. ASME **119**, 205 (1997).
[23] T. G. Fox and P. J. Flory, J. Appl. Phys. **21**, 581 (1950).
[24] A. K. Doolittle, J. Appl. Phys. **22**, 1471 (1951).
[25] M. H. Cohen and D. Turnbull, J. Chem. Phys. **31**, 1164 (1959).
[26] D. Turnbull and M. H. Cohen, J. Chem. Phys. **34**, 120 (1961).
[27] D. M. Colucci, G. B. McKenna, J. J. Filliben, A. Lee, D. B. Curliss, K. B. Bowman, and J. D. Russell, J. Polym. Sci. Pol. Phys. **35**, 1561 (1997).
[28] C. Bauwens-Crowet, J. Mater. Sci. **8**, 968 (1973).
[29] J. H. Gibbs and E. A. DiMarzio, J. Chem. Phys. **28**, 373 (1958).
[30] M. Goldstein, J. Chem. Phys. **39**, 3369 (1963).
[31] M. Naoki and S. Koeda, J. Phys. Chem. **93**, 948 (1989).
[32] G. Adam and J. H. Gibbs, J. Chem. Phys. **43**, 139 (1965).
[33] R. C. Tolman, J. Am. Chem. Soc. **42**, 2506 (1920).
[34] H. Eyring, J. Chem. Phys. **3**, 107 (1935).
[35] M. G. Evans and M. Polanyi, Trans. Faraday Soc. **21**, 875 (1935).
[36] C. A. Angell and S. Borick, J. Non-Cryst. Solids **307-310**, 393 (2002).
[37] O. Yamamuro, I. Tsukushi, A. Lindqvist, S. Takahara, M. Ishikawa, and T. Matsuo, J. Phys. Chem. B **102**, 1605 (1998).
[38] R. Richert and C. A. Angell, J. Chem. Phys. **108**, 9016 (1998).
[39] J. H. Magill, J. Chem. Phys. **47**, 2802 (1967).
[40] W. T. Laughlin and D. R. Uhlmann, J. Phys. Chem. **76**, 2317 (1972).
[41] S. Samanta, O. Yamamuro, and R. Richert, Thermochim. Acta **636**, 57 (2016).
[42] S. Samanta and R. Richert, J. Phys. Chem. B **120**, 7737 (2016).
[43] R. Richert, J. Chem. Phys. **146**, 064501 (2017).
[44] J. M. Caruthers, D. B. Adolf, R. S. Chambers, and P. Shrikhande, Polymer **45**, 4577 (2004).
[45] D. B. Adolf, R. S. Chambers, and J. M. Caruthers, Polymer **45**, 4599 (2004).

[46] G. A. Medvedev and J. M. Caruthers, J. Rheol. **57**, 949 (2013).
[47] G. A. Medvedev and J. M. Caruthers, in *Polymer Glasses*, edited by C. B. Roth (Taylor & Francis Books London, 2016), pp. 453.
[48] I. B. Rabinovich, N. V. Novoselova, E. M. Moseeva, A. G. Babinkov, and L. Y. Tsvetkova, Russ. J. Phys. Chem. **59**, 1266 (1985).
[49] C. A. Angell and D. L. Smith, J. Phys. Chem. **86**, 3045 (1982).
[50] S. V. Aditchtev, S. Benkhof, T. Blochowicz, V. N. Novikov, E. A. Rossler, C. Tschirwitz, and J. Wiedersich, Phys. Rev. Lett. **88**, 055703 (2002).
[51] D. W. Scott, W. N. Hubbard, J. F. Messerly, S. S. Todd, I. A. Hossenlopp, W. D. Good, D. R. Douslin, and J. P. McCullough, J. Phys. Chem. **67**, 680 (1963).
[52] U. Gaur and B. Wunderlich, J. Phys. Chem. Ref. Data **10**, 119 (1981).
[53] O. van den Berg, W. G. F. Sengers, W. F. Jager, S. J. Picken, and M. Wubbenhorst, Macromolecules **37**, 2460 (2004).
[54] O. Haida, H. Suga, and S. Seki, J. Chem. Thermodynamics **9**, 1113 (1977).
[55] S. Benkhof, A. Kudlik, T. Blochowicz, and E. A. Rossler, J. Phys.-Condens. Mat. **10**, 8155 (1998).
[56] Y. Z. Chua, A. R. Young-Gonzales, R. Richert, M. D. Ediger, and C. Schick, J. Chem. Phys. **147**, 014502 (2017).
[57] M. Mizukami, H. Fujimori, and M. Oguni, Prog. Theor. Phys. Supp. **126**, 79 (1997).
[58] See Supplemental Material at [URL will be inserted by publisher] for analysis of 21 materials given in Fig. 3 and Table 1 using the mobility and heat capacity data; references to original papers are provided.
[59] J. N. Andrews and A. R. Ubbelodhe, Proc. R. Soc. London, Ser. A **228**, 435 (1955).
[60] M. Cukierman, J. W. Lane, and D. R. Uhlmann, J. Chem. Phys. **59**, 3639 (1973).
[61] R. J. Greet and D. Turnbull, J. Chem. Phys. **46**, 1243 (1967).
[62] E. McLaughlin and A. R. Ubbelodhe, Trans. Faraday Soc. **54**, 1804 (1958).
[63] R. Richert, J. Chem. Phys. **123**, 154502 (2005).
[64] N. Petzold and E. A. Rossler, J. Chem. Phys. **133**, 124512 (2010).
[65] S. S. Chang and A. B. Bestul, J. Chem. Phys. **56**, 503 (1972).
[66] L. Carpentier, R. Decressain, and M. Descamps, J. Chem. Phys. **121**, 6470 (2004).
[67] C. Dreyfus, A. Aouadi, R. M. Pick, T. Berger, A. Patkowski, and W. Steffen, J. Phys.-Condens. Mat. **11**, A139 (1999).
[68] S. A. Hutcheson and G. B. McKenna, J. Chem. Phys. **129**, 074502 (2008).
[69] M. Cutroni and A. Mandanici, J. Chem. Phys. **114**, 7124 (2001).
[70] A. Mandanici, M. Cutroni, and R. Richert, J. Chem. Phys. **122**, 084508 (2005).
[71] A. Aouadi, C. Dreyfus, M. Massot, R. M. Pick, T. Berger, W. Steffen, A. Patkowski, and C. Alba-Simionesco, J. Chem. Phys. **112**, 9860 (2000).
[72] H. Svajdlenkova, A. Ruff, P. Lunkenheimer, A. Loidl, and J. Bartos, J. Chem. Phys. **147**, 084506 (2017).
[73] C. Alba-Simionesco, J. Fan, and C. A. Angell, J. Chem. Phys. **110**, 5262 (1999).
[74] L. M. Meva'a and A. Lichanot, Thermochim. Acta **158**, 335 (1990).
[75] M. Hatase, M. Hanaya, T. Hikima, and M. Oguni, J. Non·Cryst. Solids **307-310**, 257 (2002).
[76] I. A. Vasil'ev, A. D. Korkhov, D. M. Minkin, I. B. Rabinovich, M. S. Sheiman, and V. P. Nistratov, Termodin. Org. Soedin. **5**, 21 (1976).
[77] H. Fujimori and M. Oguni, J. Chem. Thermodynamics **26**, 367 (1994).
[78] A. Bondeaux and J. Huck, J. Phys. (Paris) **46**, 1717 (1985).
[79] W. M. Du, G. Li, H. Z. Cummins, M. Fuchs, J. Toulouse, and L. A. Knauss, Phys Rev E **49**, 2192 (1994).
[80] U. Schneider, P. Lunkenheimer, R. Brand, and A. Loidl, Phys Rev E **59**, 6924 (1999).
[81] F. Qi, K. U. Schug, S. Dupont, A. Döß, R. Böhmer, H. Sillescu, H. Kolshorn, and H. Zimmermann, J. Chem. Phys. **112**, 9455 (2000).

[82] G. E. Gibson and W. F. Giauque, J. Am. Chem. Soc. **45**, 93 (1923).
[83] A. Otsubo, T. Haseda, and E. Kanda, Sci. Rep. Res. Tohoku A **7**, 338 (1955).
[84] J. F. Counsell, E. B. Lees, and J. F. Martin, J. Chem. Soc. A, 1819 (1968).
[85] S. Takahara, O. Yamamuro, and H. Suga, J. Non·Cryst. Solids **171**, 159 (1994).
[86] P. G. Tait, in *Report on the scientific results of the voyage of H.M.S. Challenger during the years 1873-76. Physics and chemistry. Vol. 2* (HMSO, London, 1888), pp. 1.
[87] C. M. Roland, S. Hensel-Bielowka, M. Paluch, and R. Casalini, Rep. Prog. Phys. **68**, 1405 (2005).
[88] R. Casalini, S. S. Bair, and C. M. Roland, J. Chem. Phys. **145**, 064502 (2016).
[89] G. Fytas, T. Dorfmuller, and C. H. Wang, J. Phys. Chem. **87**, 5041 (1983).
[90] M. Naoki, H. Endou, and K. Matsumoto, J. Phys. Chem. **91**, 4169 (1987).
[91] H. Leyser, A. Schulte, W. Doster, and W. Petry, Phys. Rev. B **51**, 5899 (1995).
[92] K. U. Schug, H. E. King Jr., and R. Bohmer, J. Chem. Phys. **109**, 1472 (1998).
[93] T. Atake and C. A. Angell, J. Phys. Chem. **83**, 3218.
[94] M. G. Broadhurst, J. Res. Natl. Bur. Stand. Sec. A **66**, 241 (1962).
[95] M. G. Broadhurst, J. Res. Natl. Bur. Stand. Sec. A **67**, 233 (1963).
[96] W. Kauzmann, Chem. Rev. **43**, 219 (1948).
[97] G. Floudas, M. Paluch, A. Grzybowski, and K. L. Ngai, in *Molecular Dynamics of Glass-Forming Systems. Effects of Pressure* (Springer, Berlin, Heidelberg, 2011), pp. 39.
[98] L. D. Landau and E. M. Lifshitz, *Electrodynamics of Continuous Media* (Pergamon Press, Oxford, 1984), 2nd edn.
[99] L. Berthier and G. Biroli, Rev. Mod. Phys. **83**, 587 (2011).
[100] C. W. Gardiner, *Handbook of Stochastic Methods* (Springer - Verlag, 1985), Vol. 13, Springer Series in Synergetics.
[101] J. W. Gibbs, *Elementary Principles in Statistical Mechanics* (Charles Scribner' Sons, New York, 1902).